Morphology and structure of *Homo erectus* humeri from Zhoukoudian, Locality 1 (#20899)

First submission

Please read the **Important notes** below, the **Review guidance** on page 2 and our **Standout reviewing tips** on page 3. When ready **submit online**. The manuscript starts on page 4.

Important notes

Editor and deadline

Philip Reno / 22 Oct 2017

Files	4 Figure file(s) 4 Table file(s) 1 Raw data file(s) Please visit the overview page to **download and review** the files not included in this review PDF.
Declarations	No notable declarations are present

Review guidelines

Please read in full before you begin

How to review

When ready **submit your review online**. The review form is divided into 5 sections. Please consider these when composing your review:

1. **BASIC REPORTING**
2. **EXPERIMENTAL DESIGN**
3. **VALIDITY OF THE FINDINGS**
4. General comments
5. Confidential notes to the editor

You can also annotate this PDF and upload it as part of your review

To finish, enter your editorial recommendation (accept, revise or reject) and submit.

BASIC REPORTING

- Clear, unambiguous, professional English language used throughout.
- Intro & background to show context. Literature well referenced & relevant.
- Structure conforms to **PeerJ standards**, discipline norm, or improved for clarity.
- Figures are relevant, high quality, well labelled & described.
- Raw data supplied (see **PeerJ policy**).

EXPERIMENTAL DESIGN

- Original primary research within **Scope of the journal**.
- Research question well defined, relevant & meaningful. It is stated how the research fills an identified knowledge gap.
- Rigorous investigation performed to a high technical & ethical standard.
- Methods described with sufficient detail & information to replicate.

VALIDITY OF THE FINDINGS

- Impact and novelty not assessed. Negative/inconclusive results accepted. *Meaningful* replication encouraged where rationale & benefit to literature is clearly stated.
- Data is robust, statistically sound, & controlled.
- Conclusions are well stated, linked to original research question & limited to supporting results.
- Speculation is welcome, but should be identified as such.

The above is the editorial criteria summary. To view in full visit **https://peerj.com/about/editorial-criteria/**

7 Standout reviewing tips

The best reviewers use these techniques

Tip	*Example*
Support criticisms with evidence from the text or from other sources	*Smith et al (J of Methodology, 2005, V3, pp 123) have shown that the analysis you use in Lines 241-250 is not the most appropriate for this situation. Please explain why you used this method.*
Give specific suggestions on how to improve the manuscript	*Your introduction needs more detail. I suggest that you improve the description at lines 57- 86 to provide more justification for your study (specifically, you should expand upon the knowledge gap being filled).*
Comment on language and grammar issues	*The English language should be improved to ensure that your international audience can clearly understand your text. I suggest that you have a native English speaking colleague review your manuscript. Some examples where the language could be improved include lines 23, 77, 121, 128 – the current phrasing makes comprehension difficult.*
Organize by importance of the issues, and number your points	*1. Your most important issue* *2. The next most important item* *3. …* *4. The least important points*
Give specific suggestions on how to improve the manuscript	*Line 56: Note that experimental data on sprawling animals needs to be updated. Line 66: Please consider exchanging "modern" with "cursorial".*
Please provide constructive criticism, and avoid personal opinions	*I thank you for providing the raw data, however your supplemental files need more descriptive metadata identifiers to be useful to future readers. Although your results are compelling, the data analysis should be improved in the following ways: AA, BB, CC*
Comment on strengths (as well as weaknesses) of the manuscript	*I commend the authors for their extensive data set, compiled over many years of detailed fieldwork. In addition, the manuscript is clearly written in professional, unambiguous language. If there is a weakness, it is in the statistical analysis (as I have noted above) which should be improved upon before Acceptance.*

Morphology and structure of *Homo erectus* humeri from Zhoukoudian, Locality 1

Song Xing [Corresp., 1], **Kristian J Carlson** [2], **Pianpian Wei** [3], **Jianing He** [4], **Wu Liu** [1]

[1] Department of Paleoanthropology, Institute of Vertebrate Paleontology and Paleoanthropology, Chinese Academy of Sciences, Beijing, China

[2] Department of Integrative Anatomical Sciences, Keck School of Medicine, University of Southern California, Los Angeles, United States of America

[3] School of Life Sciences, Fudan University, Shanghai, China

[4] School of Archaeology and Museology, Peking University, Beijing, China

Corresponding Author: Song Xing
Email address: xingsong@ivpp.ac.cn

Objective: The current study reports the first humeral rigidity and strength properties of East Asian *H. erectus* in placing its diaphyseal robusticity into broader regional and temporal contexts.

Materials and Methods: We estimate true cross-sectional properties of Zhoukoudian Humerus II and quantify new diaphyseal properties of Humerus III using high resolution computed tomography. Comparative data for African *H. erectus* and Eurasian Late Pleistocene *H. sapiens* were assembled, and new data were generated from two modern Chinese populations.

Results: Differences between East Asian and African *H. erectus* were inconsistently expressed in humeral cortical thickness. In contrast, East Asian *H. erectus* consistently exhibited greater humeral robusticity compared to African *H. erectus* when standardizing properties by the product of estimated body mass and humeral length. East Asian *H. erectus* humeri typically differed less from those of side-matched Late Pleistocene hominins (e.g., Neanderthals and more recent Upper Paleolithic modern humans) compared to African *H. erectus*, but still often fell in the lower range of Late Pleistocene humeral rigidity or strength properties. Modern *H. sapiens* from China (i.e., Datong and Junziqing groups) often equalled or exceeded East Asian *H. erectus* in length-standardized properties, suggesting modern human-like robusticity of Humerus II and Humerus III.

Discussion: Even after attempting to control for potential differences in body size and limb proportions, East Asian *H. erectus* humeri exhibited greater measures of diaphyseal robusticity than an African *H. erectus* humerus. Quantitative comparisons indicate that regional variability in humeral midshaft robusticity may characterize *H. erectus* to a greater extent than presently recognized. This may suggest a temporal difference within *H. erectus*, or possibly different ecogeographical trends and/or upper limb loading patterns across the taxon. Discovery and analysis of more adult *H. erectus* humeri is critical to further evaluating and potentially distinguishing between these possibilities.

Title: Morphology and structure of *Homo erectus* humeri from Zhoukoudian, Locality 1

Author names: Song Xing[1*], Kristian J. Carlson[2,3*], Pianpian Wei[4], Jianing He[5], Wu Liu[1]

Author affiliations: [1] Key Laboratory of Vertebrate Evolution and Human Origins of Chinese Academy of Sciences, Institute of Vertebrate Paleontology and Paleoanthropology, Chinese Academy of Sciences, Beijing 100044, China; [2]Department of Integrative Anatomical Sciences, Keck School of Medicine, University of Southern California, Los Angeles, CA, USA; [3]Evolutionary Studies Institute, University of the Witwatersrand, Johannesburg, WITS 2050, South Africa; [4]State Key Laboratory of Genetic Engineering and Ministry of Education Key Laboratory of Contemporary Anthropology, School of Life Sciences, Fudan University, Shanghai 200433, China; [5]School of Archaeology and Museology, Peking University, Beijing 100871, China.

Author email addresses: SX (xingsong@ivpp.ac.cn), KJC (kristian.carlson@usc.edu), PW (weipianpian@ivpp.ac.cn), JH (hejianing@pku.edu.cn), WL (liuwu@ivpp.ac.cn)

***Corresponding Authors:** Song Xing and Kristian J. Carlson

ABSTRACT

Objective: The current study reports the first humeral rigidity and strength properties of East Asian *H. erectus* in placing its diaphyseal robusticity into broader regional and temporal contexts.

Materials and Methods: We estimate true cross-sectional properties of Zhoukoudian Humerus II and quantify new diaphyseal properties of Humerus III using high resolution computed tomography. Comparative data for African *H. erectus* and Eurasian Late Pleistocene *H. sapiens* were assembled, and new data were generated from two modern Chinese populations.

Results: Differences between East Asian and African *H. erectus* were inconsistently expressed in humeral cortical thickness. In contrast, East Asian *H. erectus* consistently exhibited greater humeral robusticity compared to African *H. erectus* when standardizing properties by the product of estimated body mass and humeral length. East Asian *H. erectus* humeri typically differed less from those of side-matched Late Pleistocene hominins (e.g., Neanderthals and more recent Upper Paleolithic modern humans) compared to African *H. erectus*, but still often fell in the lower range of Late Pleistocene humeral rigidity or strength properties. Modern *H. sapiens* from China (i.e., Datong and Junziqing groups) often equalled or exceeded East Asian *H. erectus* in length-standardized properties, suggesting modern human-like robusticity of Humerus II and Humerus III.

Discussion: Even after attempting to control for potential differences in body size and limb proportions, East Asian *H. erectus* humeri exhibited greater measures of diaphyseal robusticity than an African *H. erectus* humerus. Quantitative comparisons indicate that regional variability

in humeral midshaft robusticity may characterize *H. erectus* to a greater extent than presently recognized. This may suggest a temporal difference within *H. erectus*, or possibly different ecogeographical trends and/or upper limb loading patterns across the taxon. Discovery and analysis of more adult *H. erectus* humeri is critical to further evaluating and potentially distinguishing between these possibilities.

Keywords: East Asia; Pleistocene; hominin; upper limb; diaphyseal robusticity

INTRODUCTION

Homo erectus has been portrayed as a geochronologically persistent taxon encompassing a great deal of regional diversity over its evolutionary history (*Antón, 2003*). The initial appearance of *H. erectus* in the hominin fossil record is approximately 1.9 Ma from Koobi Fora, Kenya, while the prolonged occurrence documented in East Asia is unmatched elsewhere (*Dubois, 1894, 1936; Black, 1930, 1933; von Koenigswald, 1936, 1940, 1951; Weidenreich, 1938, 1941, 1943; Woo, 1964, 1966; Chiu et al., 1973; Hu, 1973; Jacob, 1973; Santa Luca, 1980; Wu & Dong, 1982; Wu & Poirier, 1995; Antón, 2003; Kaifu et al., 2005a, b; Liu et al., 2005; Zhu et al., 2008; Zaim et al., 2011*). Characterization of the taxon as regionally diverse emphasizes craniodental features (*Rightmire, 1998; Antón, 2003; Kaifu et al., 2005a, b; Baab, 2008; Lordkipanidze et al. 2013; Antón et al., 2016*) in focusing on hominin systematics (*Howells, 1980; Stringer, 1984; Rightmire, 1993; Wood, 1994; Antón, 2002, 2003*) and feeding behaviour (*Ungar et al., 2006*). By comparison, emphasis on *H. erectus* postcrania is less frequent when framing *H. erectus* diversity (*Ruff, 2008; Pontzer et al. 2010; Puymerail et al., 2012; Ruff et al., 2015*).

Relative scant attention given to regional diversity in *H. erectus* postcranial fossils, in part, is a function of the paucity of Asian sites preserving postcranial fossils (*Antón, 2003*); upper limb elements of East Asian hominins, such as humeri, have been recovered only from Zhoukoudian (see *Weidenreich, 1941*). As a result, current depictions of *H. erectus* postcranial morphology draw heavily from the more abundant African, Georgian, and to a lesser extent Southeast Asian, *H. erectus* fossils (e.g., *Ruff, 2008; Pontzer et al., 2010; Puymerail et al., 2012, Ruff et al. 2015*), including a relatively complete immature skeleton, KNM-WT 15000 (*Walker &Leakey, 1993*), and a partial adult skeleton from Kenya, KNM-ER 1808 (*Walker et al., 1982;*

Leakey & Walker, 1985), and sets of postcranial fossils from multiple individuals represented at Dmanisi (*Lordkipanidze et al., 2007; Pontzer et al., 2010*). Characterization of postcranial regional diversity in *H. erectus*, therefore, would benefit from expanding upon these efforts to include East Asian fossils. The aim of the present study is to broaden current understanding of regional diversity in *H. erectus* by conducting the first quantitative investigation of diaphyseal strength properties in the East Asian *H. erectus* humerus.

Cross-sectional geometric properties of long bone diaphyses provide a useful means of inferring activity patterns in past populations (*Ruff et al., 1993; Trinkaus et al., 1994; Trinkaus 1997; Stock, 2006; Carlson et al., 2007; Ruff, 2008; Carlson & Marchi, 2014; Ruff & Larsen, 2014, and references therein; Sládek et al., 2016*), although these inferences are not always straightforward (*Pearson & Lieberman, 2004; Ruff et al., 2006; Wallace et al., 2012*). Relatively recent temporal declines in humeral diaphyseal robusticity from archaic *H. sapiens* to modern *H. sapiens* have been well-documented across Eurasia and Africa (*Ruff et al., 1993; Trinkaus et al., 1994; Trinkaus, 1997*). Likewise, marked bilateral asymmetry in humeral strength appears to have emerged in and been more consistently expressed by Eurasian Late Pleistocene hominins compared to those of the Holocene, which is when presumed activity-related reductions have been hypothesized (*Trinkaus et al., 1994; Sládek et al., 2016; Sparacello et al., in press*).

Extending these humeral robusticity trends deeper into the Pleistocene hominin record (e.g., *H. erectus*) has proven more challenging, among other reasons, due to the relative incompleteness of the fossil record. Based on initial work, humeral strength of African *H. erectus* (i.e., polar section modulus) appears to fit squarely within modern human levels of overall humeral strength (*Ruff, 2008*: Fig. 2). A similar quantitative assessment of Asian *H. erectus* humeral strength has not yet been performed, although levels of skeletal robusticity in

more recent Late Pleistocene hominins from Asia have been carefully quantified and evaluated (*Shackelford, 2007; Shang & Trinkaus, 2010; Sparacello et al., in press*). To date, evaluation of humeral strength in East Asian *H. erectus* still relies largely on the original descriptions of Zhoukoudian Humerus I and Humerus II published by *Weidenreich (1938, 1941)*, who remarked upon the slenderness of the Humerus II shaft along with comparably more prominent muscle markings on its external surface relative to modern human humeri. As with *H. erectus* femora from Zhoukoudian, *Weidenreich (1938, 1941)* noted absolutely thicker cortical bone and narrower (circular) medullary canals in *H. erectus* humeri as evidence of stouter shafts compared to those of modern humans. *Weidenreich (1941:57)* also portrayed differences in robusticity between Zhoukoudian and modern human humeral shafts as less than differences between their femoral shafts, even suggesting that Zhoukoudian *H. erectus* fell within the range of modern human variability in humeral robusticity.

Subsequent to the seminal descriptions of *Weidenreich (1941)*, a third partial hominin humerus (PA64, Humerus III) was recovered from Zhoukoudian Locality 1 and attributed to *H. erectus* (*Woo & Chia, 1954*). In assessing all three humeral fossils from Zhoukoudian, *Antón (2003)* made broad qualitative comparisons to approximately 1 Ma older African *H. erectus* humeri, namely those of KNM-ER 1808 and KNM-WT 15000. *Antón (2003: 151)* noted a narrower external breadth at the midshaft in Zhoukoudian humeri, presumably based on Humerus II and Humerus III, and that Humerus II was "equally long, and exhibits the typically thick cortical walls and reduced medullary cavity seen in African *H. erectus* fossils." This characterization echoed the determination of *Weidenreich (1941)*, in part, in suggesting that humeral structure of East Asian and African *H. erectus* differed from that of modern humans in similar ways (i.e., thicker cortical bone and narrower medullary cavities). What remains

unknown, however, is whether a quantitative evaluation of humeral rigidity and strength in East Asian and African *H. erectus* can corroborate this suggested equivalence, and whether humeri from Zhoukoudian *H. erectus* may be truly modern-human like in their diaphyseal robusticity (i.e., relative humeral rigidity and strength).

The goals of the present study are threefold. First, we provide the initial quantitative assessment of humeral rigidity and strength in East Asian *H. erectus*. Second, these new data will permit the first quantitative comparisons of humeral rigidity and strength in East Asian versus African *H. erectus*, which will contribute to an improved understanding of postcranial robusticity and variability within the taxon overall, much as recent investigations of *H. erectus* lower limb elements have (e.g., *Puymerail et al. 2012; Ruff et al. 2015*). Specifically, we address whether East Asian and African *H. erectus* humeral diaphyses are similar in cortical thickness and medullary cavity dimensions. In addition to this, we address whether East Asian and African *H. erectus* humeral diaphyses are similar in relative rigidity and strength. Comparisons between humeri of Zhoukoudian *H. erectus*, more recent Late Pleistocene Eurasian hominins, and two modern Chinese populations are also undertaken in order to better frame potential uniqueness of Zhoukoudian humeral robusticity. Third, by including two modern Chinese populations that would be expected to exhibit similar latitudinal trends in ecomorphological body and limb proportions as earlier hominins from East Asia, we address whether East Asian *H. erectus* may exhibit suggested modern human-like humeral robusticity. In addition to providing new internal structural data for Zhoukoudian Humerus II and Humerus III, we provide a new detailed description of Humerus III surface morphology. This is intended to complement earlier descriptions of Humerus I and II by *Weidenreich (1941)*, and to supplement an initial description of Humerus III by *Woo & Chia (1954)*. Ultimately, the current study provides an opportunity to

begin to place East Asian *H. erectus* humeral robusticity into broader temporal and regional hominin contexts.

MATERIAL AND METHODS

The site of Zhoukoudian consists of a series of limestone caves approximately 50km southwest of Beijing. It is situated in a transitional region between mountains and plains (*Xie et al., 1985; Zhang, 2004*). Excavations at Zhoukoudian Cave, Locality 1 were performed between 1921 and 1973. Dating Locality 1 has been attempted on several occasions using a variety of methods; adding the most recent cosmogenic efforts generates a potential estimated range of 0.68 Ma to 0.78 Ma (*Shen et al., 2009*). The Middle Pleistocene landscape of the immediate area was generally similar to the present landscape. Sporopollen and sediment analyses, as well as faunal composition, suggest that the surrounding area was mainly covered by forest and steppe, with each of these being alternately dominant over the course of the Zhoukoudian hominin occupation (*Zhang & Tang, 2007*). Hominins are thought to have occupied the cave itself, or lived near its opening in a rockshelter during the Middle Pleistocene, but the overall range of cave use is uncertain (*Binford et al., 1985; Weiner et al., 1998; Wu, 1999*).

A majority of original Zhoukoudian postcranial fossils disappeared in the 1940's, and are represented today either by descriptions (e.g., *Weidenreich, 1941, 1943*) or casts produced by Weidenreich. *Weidenreich (1941)* described two humeral specimens from Zhoukoudian Locality 1 (Humerus I and II), noting their general external rugosity compared to modern humans. Neither partial humerus was associated with other skeletal elements, although *Weidenreich (1941: Table 1)* raised the possibility that Humerus II could have been associated with femur 330 (Femur III).

Weidenreich (1941) described Humerus I (specimen 81) as an unweathered small fragment of a left humerus, preserving a sharp lateral supracondylar ridge and adjoining parts of the anterolateral and posterior surfaces near the lateral margin of the olecranon fossa (see *Weidenreich, 1941*: Figs 27-29). Based largely on the sharpness of its lateral supracondylar ridge, *Weidenreich (1941)* attributed Humerus I to a male individual. *Weidenreich (1941)* described Humerus II (specimen 319) as a substantial part of a left humeral diaphysis with irregular breaks through the shaft approximately 20 – 30 mm distal to its surgical neck and 55 mm proximal to its epicondyles (*Weidenreich, 1941*: *Figs 30-32)*. *Weidenreich (1941)* noted its robusticity and sharp surface contours, attributing it also to a male individual. *Weidenreich (1941: Fig. 31)* incorporated the more fragmentary Humerus I in his reconstruction of Humerus II, which he justified by pointing towards their similar external appearance and preserved proportions, arriving at a reconstructed maximum length of 324 mm for the composite left humerus.

Description of Zhoukoudian partial humerus (PA 64, Humerus III)

In 1951, a third partial hominin humerus (PA64, Humerus III) was discovered at Zhoukoudian Locality 1 and attributed to *H. erectus* (Woo and Chia, 1954). Humerus III is a right humeral shaft fragment, approximately 108.2 mm in its maximum dimension (Fig. 1). It is grayish-black in color, retains a well-preserved surface, and exhibits a number of anatomical details. It is unclear whether the external color is due to intentional burning, or some unknown diagenetic process (e.g., mineral staining), although it is worth noting that *Weidenreich (1938, 1941)* describes other hominin material from the site as burnt (e.g., Femur II). *Woo & Chia*

186 *(1954)* suggested that Humerus III represents the middle-third of a diaphysis, which we can
187 confirm based on our observed similarities between its retained morphology and overlapping
188 regions of the mirrored composite Humerus II rendering (Fig. 1). However, while the midshaft
189 region is preserved on Humerus III, not enough of its diaphysis is retained to allow us to
190 similarly evaluate the distinctive presence of a Humerus II-like "heavy" proximal half with an
191 "almost circular" external contour and a "slender" distal half with a "triangular" contour
192 (*Weidenreich, 1941: 55*).

193 *Woo & Chia (1954)* noted that overall muscle attachment sites on the external surface are
194 generally not rugose, nor is the shaft particularly robust (Fig. 1). We generally agree. Overall, the
195 preserved surface of Humerus III does not recall to us the same level of rugosity as described by
196 *Weidenreich (1941)* for the original Humerus II diaphysis, or as is evident on a cast of the
197 composite reconstruction made by Weidenreich (see Fig. S1). Humerus III also has distinctly
198 different cortical thickness and medullary cavity dimensions compared to those attributed to
199 Humerus II (*Weidenreich, 1941*: Fig. 58) and estimated in the present study (see Fig. 2). While
200 this could indicate that Humerus III is from a non-adult individual, we find this less likely based
201 on external dimensions of its cross-sections (Fig. 2). Rather, it would seem more likely to us that
202 Humerus III may represent a less robust adult male compared to Humerus II, or perhaps an adult
203 female.

204 Insert Figure 1 here

205 The proximal break through the shaft of Humerus III is irregular and runs oblique to the
206 longitudinal axis of the shaft (Fig. 1). It passes through the inferior region of the deltoid
207 tuberosity on its anterolateral surface, while posteriorly it extends further proximally. On the

medial side of Humerus III, the break extends distally until reaching the mid-anterior surface and extends proximally until reaching the mid-posterior surface of the diaphysis. Along its inferiormost extent, the proximal break runs transversely across the anterior surface of the diaphysis until reaching the lateral surface. Inferior to this section of the break, the deltoid tuberosity continues for approximately 14 mm. Overall, the lateral side of the proximal break recalls the general appearance of its medial side. *Woo and Chia (1954)* suggested a section of the proximal break is fresh, implying excavation damage. The distal break through the shaft is also irregular and runs oblique to the longitudinal axis of the shaft (Fig. 1). Its form mirrors the proximal break in extending more distally on the anterior surface and more proximally on the posterior surface. The transverse section of the distal break, however, is on the posterior surface of Humerus III whereas the transverse section of the proximal break is on its anterior surface. Posteriorly, the distal break extends proximally until immediately beneath the level of the nutrient foramen, while it extends well inferior to the nutrient foramen on the anterior surface.

The deltoid tuberosity of Humerus III does not exhibit the same double-ridged form with an intervening depression that *Weidenreich (1941)* describes for Humerus II. Rather, it is a single, continuous anterolaterally-facing swelling of the diaphysis without an intrusive depression. It creeps around the lateral side of the shaft until it is visible in posterior view. This uninterrupted form may be due to only its inferior portion being preserved on Humerus III, as even the double-ridged structure of Humerus II converges into a single structure inferiorly (*Weidenreich, 1941*). Alternatively, it may indicate comparatively less rugosity of the insertion site for *m. deltoideus* on Humerus III compared to Humerus II. This latter possibility would be consistent with the other noted differences between Humerus II and Humerus III in terms of general surface rugosity, cortical thickness, and medullary cavity dimensions.

The anterior surface of the Humerus III shaft is convexly rounded with a maximum point of curvature immediately lateral to its central region (Figure 1). Medially, the anterior surface gently slopes towards a rounded border separating it from the posterior surface. Contiguous flatness of the anteromedial border is greater in Humerus III than that portrayed in Humerus II (*Weidenreich, 1941*). On the medial border of Humerus III, a nutrient foramen lies immediately beneath the confluence of two diverging ridges extending distal to it on either side. Were these not interrupted by the distal break, they would seem to continue distally as the anterior and posterior rims of the medial supracondylar ridge. The foramen opens superiorly into a shallow groove that extends proximally for a few millimeters in length along the shaft. There is no distinct rugosity indicating the location of the *m. brachialis* origin on Humerus III.

The posterior surface of the Humerus III diaphysis is less rounded than its anterior surface (Fig. 1). Superiorly, the posterior surface faces predominantly posteriorly, while inferiorly it transitions to facing comparatively more medially. Posterior and inferior to the deltoid tuberosity, a radial groove can be palpated, but not easily distinguished by eye. It continues proximally along the shaft until it is ultimately interrupted by the proximal break, while distally it gradually dissipates into the anterolateral surface. The inferior extent of the origin of the lateral head of *m. triceps brachii* appears as a subtly protruding triangular area on the posterior surface, measuring 6 mm in mediolateral breadth at its widest point. While this area is interrupted by the proximal break, its rounded edges converge distally into a single ridge. A visible ridge on the proximolateral surface, immediately inferior to the radial groove, appears to define the origin of the medial head of *m. triceps brachii*. The ridge courses proximomedially to distolaterally across the posterior surface. At the level of the nutrient foramen, the ridge is interrupted on the lateral surface by the distal break. Medially on the shaft, a comparatively

subtler ridge follows a parallel course for 7 mm, becoming defined only in the distal half of the preserved shaft. This latter ridge demarcates what eventually would appear to become the lateral supracondylar ridge. Not enough of this ridge is preserved in Humerus III, however, to make a direct form comparison to the "sharply edged" ridge attributed to Humerus I (*Weidenreich, 1941: 57*).

Comparative samples

In order to compare humeral structural properties of East Asian *H. erectus* humeri to those of adult African *H. erectus*, we calculated humeral structural properties from a published cross section of the individual represented by KNM-ER 1808 (*Ruff, 2008*). To provide a more informative contextual framework for evaluating Zhoukoudian humeral robusticity, we also compared structural properties from several Late Pleistocene Asian humeri. Levels of humeral robusticity expressed in Late Pleistocene hominins are traditionally higher than those expressed in Holocene modern humans (*Trinkaus et al., 1994; Sparacello et al., in press*). Our comparative Late Pleistocene sample included partial right and left humeri of an adult skeleton (Tianyuan 1) recently discovered at the Chinese site of Tianyuan Cave (*Tong et al., 2004*). ~~Accelerator mass spectrometry (AMS) and U-series dating on mammal teeth, and AMS radiocarbon dating on a hominin femur from Tianyuan 1, suggest that the hominin occupation at Tianyuan Cave occurred between 39-42 ka~~ (*Shang et al., 2007; Shang & Trinkaus, 2010*). Systematic study of Tianyuan 1 has noted that it generally exhibited a mixture of features characteristic of early modern humans (e.g., crural indices) and features commonly observed ~~amongst~~ archaic humans (e.g., pronounced humeral midshaft asymmetry and tibial robusticity, the latter suggesting an emphasis on

mobility) (*Shang et al., 2007; Shang & Trinkaus, 2010*). Because of pronounced humeral asymmetry in Late Pleistocene hominins from multiple regions of the world (*Sládek et al., 2016; Sparacello et al., in press*), and because the Zhoukoudian *H. erectus* sample included right and left humeri, we report separate right and left humeral properties of Tianyuan 1 and emphasize same-side comparisons when possible.

We also compiled published humeral cross-sectional data for additional Late Pleistocene Asian hominins. Specifically, we compared Late Upper Paleolithic modern humans (n = 10) from Minatogawa (individuals 1, 2, 3, 4) and Tam Hang (individuals 2, 3, 7, 11, 13, 14) (see *Sparacello et al., in press*). The Minatogawa Fissure site is on the island of Okinawa, with charcoal fragments reportedly found near the skeletal material providing two radiocarbon (^{14}C) dates of approximately 18 ka (*Baba & Narasaki, 1991; Baba et al., 1998; Kaifu et al., 2011; Matsu'ura & Kondo, 2011*). The Tam Hang rockshelter in Northern Laos has been radiocarbon (^{14}C) dated to 15.7 ka (*Shackelford & Demeter, 2012*). Tam Hang occupies an inland location and its archaeological assemblage is characteristic of the regional Hoabinhian techno-complex (*Patole-Edoumba et al., 2015*). Lower limb diaphyses of the human skeletons recovered from Tam Hang appear to be generally gracile in comparison to other Late Pleistocene hominins from East and Southeast Asia (*Shackelford, 2007*).

Finally, to further establish the contextual framework for evaluating Zhoukoudian Humerus II and Humerus III, we compiled additional published Eurasian humeral data (*Churchill, 1994; Trinkaus et al., 1994; Trinkaus & Churchill, 1999; Crevecoeur 2008; Sparacello et al., in press*) from Middle Paleolithic (n = 6), Neanderthal (n = 18), Early Upper Paleolithic (n = 25) and Late Upper Paleolithic (n = 10) hominins (see Table S1).

In addition to Late Pleistocene hominins, we acquired comparative structural properties from humeri of two recent modern Chinese populations. First, we sampled right humeri of adult individuals in the Datong population (n = 10), which lived in the Beiwei Dynasty during approximately the 5th Century (*Han, 2005*). The Datong inhabited a basin surrounded by mountainous terrain with an elevation range of 500 to 2000 m. Nitrogen isotope data indicate a diet emphasizing meat consumption, and imply a pastoral subsistence strategy with little evidence of agriculturalism (*Zhang et al., 2010*). Sex attributed to individuals is unfortunately unavailable in this sample. Second, we sampled right humeri of adult individuals in the Junziqing population of the Qing Dynasty (1736-1851) (n = 23). This recently excavated material comes from Xinxiang City, Henan, central China. Xinxiang consists of plains, and historical records indicate that an agricultural economy was dominant during the Qing Dynasty. The Junziqing sample includes 11 females and 12 males, with sex determined according to traditional cranial and pelvic osteological indicators. The Junziqing had an agricultural subsistence strategy with no evidence of animal sacrifice, weaponry, or other relics that might be associated with stock raising or a hunter-gatherer lifestyle.

Acquisition of cross-sectional properties

Humeri from Zhoukoudian *H. erectus*, the Late Pleistocene early modern human from Tianyuan Cave, and recent modern Chinese were scanned using the 450kV high resolution computed tomography facilities (designed by the Institute of High Energy Physics, Chinese Academy of Sciences) housed in the Institute of Vertebrate Paleontology and Paleoanthropology (IVPP). Scan parameters for the sample included: 380 kV, 1.5 mA, 4 frame averaging, 0.5

angular increment, and 360 degrees of rotation. Final isometric voxel size obtained for the sample was 160 µm. For each scan, there were 720 projections converted into image stacks of .RAW files using the IVPP225kVCT_Recon algorithm.

In order to quantify and compare internal structure, serial image data stacks obtained from high resolution scanning were imported into VGStudio Max 2.1 (Volume Graphics GmbH, Heidelberg, Germany). Using the region of interest tool, with a tolerance setting of 3000, we selected all voxels representing the material of interest (i.e., a fossil or modern comparative humerus). From the selected voxels, a 3D volume or region was created, and from each of these a volume rendering of an entire bone was extracted. Each volume rendering was aligned to the same vertical and horizontal axes *in silico* as have been used for physical specimens. In other words, criteria for aligning humeral volume renderings followed standard procedures used with dry bones (*Ruff, 2002a; Carlson, 2005*), and that have been adapted for use in *in silico* environments (*Carlson et al., 2008*). Briefly, the longitudinal axis of a rendered diaphysis was aligned to a vertical axis in morphospace. Next, each rendered volume was aligned to a vertical plane passing through this vertical axis by rotating the 3D rendering about its longitudinal axis, or about its midpoint (i.e., rotating end over end), until the two most anterior points of the distal epiphysis (i.e., usually on the capitulum and trochlea of the rendering, or on both rims of the trochlea of the rendering) and the most anterior projecting point on the proximal end (e.g., usually the lesser tubercle) were positioned in the same vertical plane.

Once specimens were aligned, intact diaphyseal cross sections were obtained from the rendering midshaft and saved as 16-bit TIF images (Figs 2 and S2). In order to estimate true cross-sectional properties from the diaphysis of Humerus II, we had to modify our approach. First, it is worth noting general similarity between the form of the external contour at our

343 estimated Humerus II midshaft (Fig. 2) and the form of the external contour at Weidenreich's
344 estimated Humerus II midshaft (1941: Fig. 30 I). For Humerus II cross sections (Fig. 2), we
345 estimated medullary cavity size using published descriptions and measurements of Humerus II
346 (Weidenreich, 1941), as well as an anterior view radiograph of the original fossil (*Weidenreich,*
347 *1941: Fig. 58 D*). *Weidenreich (1941)* measured medullary canal breadth of Humerus II at its
348 narrowest point (distal shaft) as 22% of transverse shaft diameter and 64% of the transverse shaft
349 diameter at its widest point (proximal shaft). *Weidenreich (1941)* also described medullary canal
350 dimensions as rapidly narrowing distal to the midshaft of Humerus II. Using *Weidenreich's*
351 *(1941: Fig. 58 D)* published radiograph of Humerus II, we measured medullary canal breadth as
352 36% of transverse shaft diameter at our estimated midshaft location (Fig. S3), which
353 corresponded to a point slightly proximal to the beginning of the prominently constricted portion
354 of the medullary canal. We use this value (36%) to proportionately rescale a medullary cavity of
355 the same general form and orientation as that observed within Humerus III, which we then
356 centered in the transverse plane of the Humerus II cross section (see Fig. 2).

357 Insert Figure 2 here

358 Because of the incomplete state of the partial right humerus from Zhoukoudian (Humerus
359 III), locating comparable, fully intact cross sections from it also required a modified approach.
360 We initially generated a mirrored rendering from the composite cast of the more complete left
361 Humerus II reconstruction (Weidenreich, 1941), using the protocol outlined above. The mirrored
362 rendering of the Humerus II composite cast was imported into VGStudio Max 2.1 (Volume
363 Graphics GmbH, Heidelberg, Germany), and aligned following the procedure described above.
364 The rendering generated from Humerus III was fit to the equivalent area of the aligned, mirrored
365 rendering of the Humerus II composite cast using external features retained on both renderings

(Fig. 1). While the original left Humerus II fossil did not retain proximal or distal articular ends, which were fully reconstructed in the composite cast of *Weidenreich (1941)*, the shaft region overlapping with Humerus III was fully intact. We estimated midshaft on Humerus III as the diaphyseal location immediately distal to the inferior edge of the deltoid tuberosity. On the more complete Humerus II composite reconstruction by *Weidenreich (1941)*, the analogous point immediately distal to the inferior edge of the deltoid tuberosity also generally approximated midshaft (see Figs 1, S1, and S3). In Datong and Junziqing comparative modern samples (n = 33), by comparison, all humeri exhibited an inferiormost extent of the deltoid tuberosity between 53% and 43% of humeral length (where 0% length corresponds to the distalmost end of the diaphysis), while a majority exhibited even stronger correspondence between this anatomical landmark and midshaft (i.e., locations fell between 51% and 46% humeral length).

For both Humerus II and Humerus III (Fig. 2), we identified a second more distal location on diaphyses in an attempt to maximize comparability to the published 40% diaphyseal cross section of KNM-ER 1808, which itself was defined using an estimate of humeral length (*Ruff, 2008*). On Humerus III, we chose a location 6.3 mm distal to its estimated midshaft location taking advantage of both anatomical landmarks that could be reliably identified (e.g., the inferiormost extent of the deltoid insertion and the nutrient foramen) and the intactness of the cross section. By superimposing and aligning the Humerus II composite reconstruction (e.g., see Fig. 1), we defined an analogous position on Humerus II for a more distal cross section. Using estimates of length for the composite reconstruction of Humerus II, this more distal location corresponds to approximately 48% diaphyseal length in the Zhoukoudian humeri. Following the same estimation procedure as described above, we determined medullary cavity breadth of the more distal Humerus II cross section to be approximately 35% of its transverse external diameter

(Fig. S3). This value (35%) was used to proportionately rescale a medullary cavity of the same general form and orientation as that observed within Humerus III, which we then centered in the transverse plane of the Humerus II cross section (see Fig. 2). Ultimately, while error in estimating true cross section locations on Zhoukoudian humeri may be present, it is worth noting that general similarities between mid-diaphyseal cross-sectional properties have been observed in human humeral and femoral cross sections sampled up to 20% length apart, while variability between mid-diaphyseal cross-sectional properties has been shown to be trivial in cross sections that are approximately 5% length apart (*Sládek et al., 2010; Davies & Stock, 2014; Shaw et al., 2014; Mongle et al., 2015a, b*). Thus, given that sets of Zhoukoudian humeral cross sections are derived from 50% and 48% diaphyseal lengths, and both are distal to deltoid insertions, and given that the 40% diaphyseal length cross section of KNM-ER 1808 (*Ruff, 2008*) is based on an estimate of humeral length itself, we believe structural comparisons may be reasonably made.

Once cross sections were acquired (Fig. 2; Fig. S2), they were imported into ImageJ 1.50e (*Rasband, 2015*) where they were converted to 8-bit TIFF images and standard cross-sectional properties were calculated using the BoneJ 1.4.1 plugin (*Doube et al., 2010*). The only property not measured using the BoneJ 1.4.1 plugin (*Doube et al., 2010*) was total subperiosteal area (TA), which we measured using the magic wand tool in ImageJ 1.50e (*Rasband, 2015*). In order to pre-process the 8-bit TIFFs for use in BoneJ, a three-step process was followed. First, each image was binarized using a threshold for inclusion equal to the half-maximum gray value amongst bone pixels. Second, the endosteal border of each cross section was cleaned (e.g., trabecular struts digitally removed) following criteria outlined elsewhere (*Carlson, 2005*). Third, internal spaces between endosteal and periosteal envelopes were filled, thus creating a cross section without intracortical porosity.

412 For descriptive and comparative purposes, we report TA, cortical area (CA), percentage
413 cortical area (%CA), and principal moments of area (I_{max} and I_{min}). We calculate polar moment
414 of area (J) as the sum of I_{max} and I_{min}. We also report section moduli (Z_{max} and Z_{min}) and the polar
415 section modulus (Z_p). We select these properties, which are calculated independent of anatomical
416 axes, in recognition of the possibility that the fully reconstructed articular ends of the composite
417 cast of Humerus II may introduce an unknown amount of error when trying to precisely identify
418 AP and ML anatomical planes during the alignment procedure described above. Thus, we did not
419 calculate structural properties with respect to AP or ML anatomical planes (i.e., I_x, I_y, Z_x, and Z_y)
420 for either Humerus II or Humerus III.

421

422 *Standardization and analysis of structural properties*

423 When comparing diaphyseal cross-sectional properties of long bones across disparate
424 groups sampling different latitudes, particularly within the lower limb, it is important to
425 standardize properties by measures of body size or shape because the former may exhibit
426 allometric relationships with the latter (*Ruff et al., 1993; Ruff & Larsen, 2014*). Such
427 standardized properties are reliable and accurate measures of skeletal robusticity (see *Pearson,*
428 *2000*). Typically, body mass is the most frequently used proxy for body size (or force applied
429 when modelling beam bending), while bone length is the most frequently used proxy for beam
430 length. Thus, a measure such as the product of body mass and bone length is appropriate for
431 scaling second moments of area or the polar moment of area (*Polk et al., 2000*) and section
432 moduli (*Ruff, 2003a*) by approximating bending moments of long bones.

For specific interregional comparisons, such as those of East Asian and African *H. erectus* properties, we standardized second moments of area, polar moments of area, and section moduli using the product of estimated body mass and bone length to account for any potential ecomorphological trends in body proportions. For Humerus II and Humerus III, we derived body mass estimates using the average (53.6 kg) of multivariate body mass estimates for Femur I (54.8 kg), Femur IV (54.3 kg), and Femur VI (51.6 kg) (*Grabowski et al., 2015*). *Weidenreich (1941)* attributed Femur I, Femur IV, and Femur VI to male individuals, as he attributed the reconstructed composite cast of Humerus II. For KNM-ER 1808, we derived an estimated body mass using the average (60.2 kg) of three recently published estimates: 79 kg (*Will & Stock, 2014*), 63 kg (Antón et al., 2014: Table S2), and 38.5 kg (*Grabowski et al., 2015*). *Shang & Trinkaus (2010)* used vertical femoral head diameter and several regression formulae to calculate a range of body mass estimates for Tianyuan 1. Ultimately, they endorsed a body mass estimate of 85.1 kg for scaling limb bone structural properties of Tianyuan 1, which is the value we adopted in the present study. For Middle Paleolithic, Neanderthal, Early Upper Paleolithic, and Late Upper Paleolithic hominins, we used body mass estimates reported by *Sparacello et al. (in press)*.

Based on reasonably similar external dimensions and contours in their overlapping regions (see Figs 1 and 2), we used estimated length of the composite Humerus II reconstruction as a suitable proxy for an estimated length of Humerus III. In acknowledgement of the uncertainty that exists in estimating the length of Humerus II, and by default Humerus III, we generated three different length estimates for standardizing both sets of cross-sectional properties. For the first estimate, we used maximum length (324.0 mm) of the composite Humerus II reconstruction published by *Weidenreich (1941)* (Figs S1 and S3). *Weidenreich*

456 *(1941: 55)* remarked that the proximal end of the reconstruction "may possibly have been shorter
457 than appears in the restoration". For this reason, the estimate of Weidenreich serves as a
458 reasonable upper boundary for our range of length estimates. For the second estimate, since the
459 composite Humerus II reconstruction retained the deltoid tuberosity and the proximal border of
460 the olecranon fossa, we regressed distance between the inferiormost extent of the deltoid
461 tuberosity and the proximalmost extent of the olecranon fossa against maximum length in the
462 modern Chinese sample (n = 33; see SI Text S1, Table S2, and Figs S1 and S4). The regression-
463 derived estimate of Humerus II maximum length is 307.4 mm. Since both modern Chinese
464 groups, particularly the Junziqing, tended to have shorter humeri than other groups in the sample,
465 and notably overlapped with the upper half of the published range for the East Eurasian Late
466 Upper Paleolithic sample (Table 1), this estimate serves as a reasonable lower boundary for our
467 range of length estimates. Finally, we averaged both of these estimates to derive a third estimated
468 maximum length (315.7 mm). All three estimates were utilized separately when standardizing
469 cross-sectional properties, creating a range of lengths (16.6 mm) equal to approximately 5.3% of
470 the average length estimate (315.7 mm). For KNM-ER 1808, we used a rough approximation of
471 350 mm for its estimated length (Ruff, 2008; pers. comm). For Tianyuan 1, we used a
472 biomechanical length of the left humerus (327.4 mm) as reported by *Shang & Trinkaus (2010)*.
473 We used the same value (327.4 mm) as a proxy for length of the right humerus of Tianyuan 1,
474 which has not yet been estimated. For Middle Paleolithic, Neanderthal, Early Upper Paleolithic,
475 and Late Upper Paleolithic hominins, we used humeral lengths reported by *Sparacello et al. (in*
476 *press)*. For Datong and Junziqing recent modern human samples, we measured humeral
477 maximum length.

While some have argued that similar scaling factors should apply to the upper limb as well as the lower limb, as correlations between humeral properties and body mass have been demonstrated (*Ruff, 2000, 2003a*), others have argued on theoretical grounds that in humans upper limb loading should be less influenced by body mass than lower limb loading since the upper limbs ~~have been emancipated from locomotor involvement, i.e., habitual~~ weight-bearing (*Pearson, 2000; Carlson et al., 2007*). In the present study, since the humeral diaphysis is less likely affected by potential body breadth differences compared to the proximal femur, and since several individuals within our region-specific East Asian sample were without reliable body mass estimates (e.g., no associated femoral head measurements), we follow others who have used bone length to standardize diaphyseal properties (*Trinkaus et al., 1999*), particularly for the humerus (*Pearson, 2000; Carlson et al., 2007*). We use this protocol explicitly for comparisons between Zhoukoudian *H. erectus*, Tianyuan 1, and the modern Chinese samples where ecomorphological trends in body or limb proportions are expected to be relatively consistent. For such comparisons, we standardize cross-sectional properties to create dimensionless values as follows: total area and cortical area were divided by the square of maximum length, section moduli were divided by the third power of maximum length, and humeral principal/polar moments of area were divided by the fourth power of maximum length.

RESULTS

Are East Asian and African H. erectus humeral diaphyses similar in cortical thickness and medullary cavity dimensions?

499 The midshaft of Humerus II exhibits a similarly high estimate of %CA compared to the
500 %CA of the KNM-ER 1808 cross section, both being near the upper end of the observed
501 hominin ranges (Tables 1 and 2). The more distal cross section of Humerus II exhibits a similar
502 trend (i.e., 1.5% lower %CA than its midshaft), still exceeding the %CA of the KNM-ER 1808
503 cross section (Tables 2 and S3). The midshaft of Humerus III, on the other hand, is
504 comparatively lower in %CA, falling usually in the lower half of the observed hominin group
505 ranges (i.e., between observed group means and minimum values) (Table 1). While the more
506 distal cross section of Humerus III, like Humerus II, also exhibits an incremental difference in
507 %CA compared to its midshaft (2.0% higher: Table S3), it still usually falls in the lower half of
508 the observed hominin group ranges. Due to the similarity in %CA between the two locations,
509 only the midshaft of Humerus II and Humerus III is considered further.

510 Insert Table 1 here

511 Insert Table 2 here

512 Midshaft %CAs of both Tianyuan 1 humeri fall approximately midway between the
513 observed lower Humerus III midshaft %CA and the estimated higher Humerus II midshaft %CA,
514 as do average %CAs for the Middle Paleolithic, Neanderthal, and East Eurasian Late Upper
515 Paleolithic groups (Tables 1 and 2, Fig. 3). Average %CA of the Early Upper Paleolithic group
516 also exceeds the observed %CA of the Humerus III midshaft, although by only roughly half the
517 amount of the other Late Pleistocene hominin groups. Cognizant of the generally equivalent
518 subperiosteal areas in midshaft cross sections of Humerus II and Humerus III versus the cross
519 section of the KNM-ER 1808 humerus (i.e., differences less than 5%), thicker cortical bone and

a relatively reduced medullary cavity best characterize Humerus II and the KNM-ER 1808 humerus, while Humerus III is not equally remarkable in these characteristics.

Insert Figure 3 here

When standardizing the amount of bone in midshaft cross sections by squared humeral length (sCA: Table S4), the range of observed Humerus III values tends to fall above sCA of KNM-ER 1808. The same trend is evident when substituting the slightly greater sCA of the more distal cross section of Humerus III (Table S4). By comparison, ranges of estimated Humerus II sCAs from the midshaft (Tables S5) and more distal cross section (Tables S3) fall well above those of either of the other *H. erectus* humeri (Table S3, S5). With few exceptions, and irrespective of the estimated lengths used as scaling factors in the present study, estimated sCAs of the Humerus II midshaft fit comfortably within the upper half of observed sCA ranges for left humeri of Late Pleistocene hominins (i.e., between observed group means and maximum values) (Tables S5), while observed sCAs of the Humerus III midshaft tend to fall within the lower half of the observed sCA ranges for right humeri of Late Pleistocene hominins (i.e., between observed group means and minimum values) (Table S4). The observed sCA for the KNM-ER 1808 cross section, on the other hand, falls below the observed midshaft values of both right and left Tianyuan I humeri as well as in the lower half of the observed sCA ranges for right humeral midshafts of all other hominin groups in the study. In other words, despite the comparatively high %CA demonstrated by KNM-ER 1808 (i.e., its relatively high cortical thickness), its rather long estimated length (*Ruff, 2008*), which falls in the upper end of the range of humeral lengths for the entire comparative sample analyzed in the present study, results in relatively lower amounts of compressive rigidity compared to Zhoukoudian humeri.

Are East Asian and African H. erectus humeral diaphyses similar in relative rigidity and strength?

Despite relatively small differences between subperiosteal areas of Zhoukoudian Humerus II and Humerus III midshafts (< 3%: Tables 1 and 2), the observed differences in cortical thickness create about 15% greater unstandardized principal moments of area (I_{max} and I_{min}) and polar moments of area (J) in Humerus II (Tables 1 and 2). The latter structural differences dissipate in the more distal cross section (< 3%), being offset by a relative increase in subperiosteal area of Humerus III (Fig. 2; Table S3). This variability is noteworthy when comparing all *H. erectus* humeri. Humerus III, despite exhibiting markedly less cortical thickness than the humerus of KNM-ER 1808, still exhibits higher absolute I_{max}, J, and Z_{max} than KNM-ER 1808 (Tables 1 and S3). This indicates that Humerus III, despite its lower cortical thickness, retains comparatively more absolute rigidity or strength than the humerus of KNM-ER 1808 largely because of its relatively minor expansion in external (subperiosteal) contour. Humerus II, by comparison, exhibits comparatively greater absolute rigidity or strength both because of its cortical thickness and its slightly expanded external (subperiosteal) contour.

Standardizing structural properties results in different trends. When standardizing humeral rigidity or strength to the product of body mass and bone length, relative robusticity of Zhoukoudian humeri becomes even more apparent (Tables 3 and 4). Even the less 'thick' of the two Zhoukoudian humeri (Humerus III) consistently exceeds KNM-ER 1808 in each quantitative measure (except for the lowest range of sI_{min}) irrespective of the estimated length used in calculations for either cross section (Tables 3 and S4). Notably, KNM-ER 1808 falls near or below the lower end of comparably standardized structural properties of Late Pleistocene right humeri included in the study (Table 3).

565 Insert Table 3 here

566 Insert Table 4 here

567 The upper end of the range of Humerus III midshaft values consistently falls at or just
568 below the sI_{max}, sZ_{max}, sJ, or sZ_p of the right Tianyuan 1 humerus (Table 3 and Fig. 4), while the
569 same Humerus III ranges consistently exceed those of the less strong left Tianyuan I humerus
570 (Table 4). By comparison, ranges of sI_{max}, sZ_{max}, sJ, and sZ_p estimated from the Humerus II
571 midshaft consistently exceed those observed in either Tianyuan 1 humerus. Compared to right
572 humeri from other Late Pleistocene hominins (Table 3), the midshaft of Humerus III exhibits
573 ranges of sI_{max}, sI_{min}, and sJ that usually overlap with the lower half of observed ranges
574 (Neanderthals, Early Upper Paleolithic modern humans, East Eurasian Late Upper Paleolithic),
575 or falls below them (Middle Paleolithic; except for sI_{max}). Compared to left humeri from other
576 Late Pleistocene hominins (Table 4), the midshaft of Humerus II exhibits ranges of sI_{max}, sI_{min},
577 and sJ that overlap with the upper half of observed ranges (Neanderthals and Early Upper
578 Paleolithic modern humans), or usually falls above them (Middle Paleolithic and East Eurasian
579 Late Upper Paleolithic).

580 Insert Figure 4 here

581 *Does East Asian H. erectus exhibit modern human-like humeral robusticity compared to two*
582 *modern Chinese populations?*

583 *Weidenreich (1941)* described Zhoukoudian humeri as modern-like in their robusticity.
584 When comparing sCA of modern Chinese right humeri and Zhoukoudian humeri, the less robust
585 right Humerus III overlaps within the bottom half of sCA ranges of both groups (Table S4),
586 while the more robust left Humerus II overlaps with the upper half of sCA range of both groups

(Table S5). This overlap appears to be more attributable to the comparatively thick cortical shafts of both Zhoukoudian humeri rather than any sort of subperiosteal expansion since even the less robust Humerus III has a %CA that falls in the upper end of the ranges observed in both modern Chinese samples (Table 1).

When comparing length-standardized humeral midshaft properties used to evaluate rigidity or strength, Humerus II usually overlaps or falls below the lower half of the observed Datong ranges (i.e., between the observed group mean and minimum value), or overlaps entirely with the observed lower half of the less robust Junziqing ranges (Tables and S4). Comparing length-standardized humeral properties of the right Humerus III to the same modern Chinese right humeri indicates a generally similar trend irrespective of the estimated length used in scaling the former. While Humerus III occasionally overlaps with the observed Datong ranges, or more often falls below, it usually overlaps entirely with the observed lower half of the less robust Junziqing ranges (i.e., between the observed group mean and minimum value), and only occasionally extends below it (Table S4).

The range of humeral length estimates for Zhoukoudian Humerus II and Humerus III fall in the upper half of the observed ranges for the Datong and Junziqing samples (Tables 1 and 2). The Tianyuan 1 humeral length also falls in the upper half of the observed Datong and Junziqing humeral length ranges (Table 1). This suggests that both modern Chinese groups may have been small-bodied compared to other hominin groups in the sample, or at least appear to have had comparatively short (but still strong) humeri. Regardless of which may be the case, the range of difference exhibited by the two Zhoukoudian humeri fits within the lower half of the 2-3 fold greater range of observed length-standardized properties (i.e., observed maximum relative to minimum observed values) exhibited by these relatively small groups of modern Chinese (Tables

S4 and S5). This underscores the amount of variability that may be exhibited by modern humans, and provides quantitative support for suggested modern-like aspects of Zhoukoudian humeral robusticity (*Weidenreich, 1941*).

DISCUSSION

This study demonstrates that East Asian *H. erectus* humeri (Zhoukoudian Humerus II and Humerus III) exhibit greater humeral rigidity and strength compared to African *H. erectus* humeri (KNM-ER 1808). This difference exists whether one compares absolute values of properties or properties scaled to the product estimated body mass and humeral length. Relative to humeri of Late Pleistocene hominins from Eurasia, the 1 Ma more recent *H. erectus* humeri from Zhoukoudian, Humerus II and Humerus III, were consistently closer in robusticity than the *H. erectus* humerus, KNM-ER 1808. While we could not acquire cross sections from Humerus II and Humerus III in the precise diaphyseal location as acquired from KNM-ER 1808 (i.e., an estimated 40% length location), a second location in Zhoukoudian humeri that was distal to midshaft, and also avoided the deltoid tuberosity altogether, substantiated the midshaft comparisons. Support for comparisons of the different diaphyseal locations in the present study also comes from other studies (*Sládek et al., 2010; Davies & Stock, 2014; Shaw et al., 2014; Mongle et al., 2015a, b*) reporting general similarities between mid-diaphyseal cross-sectional properties in human humeral or femoral cross sections sampled up to 20% length apart, and that have shown mid-diaphyseal cross-sectional properties to differ trivially in cross sections that are approximately 5% length apart. Interestingly, the observed differences in diaphyseal robusticity documented in the present study occurred despite similar cortical thicknesses in KNM-ER 1808

and Humerus II and a noticeably less 'thick' diaphysis in Humerus III. This indicates that the ~~sublter~~ differences in subperiosteal area favoring Zhoukoudian humeri (i.e., periosteal expansion) were more impactful on the observed robusticity differences compared to the more markedly different cortical thicknesses.

In considering the observed humeral robusticity differences of East Asian and African *H. erectus*, a few factors warrant further discussion. The approximate 1 Ma difference between the older African and more recent East Asian *H. erectus* humeri investigated in this study may reflect temporal evolutionary trends within the taxon (apart from general body size increases) in addition to any potential regional difference in body proportions or activity levels. Discovery of contemporary *H. erectus* humeri in Africa and East Asia could help resolve this issue more definitively. In the interim, it is important to consider potential differences in body proportions across individuals from these regions since they may introduce a potential confound in comparisons of humeral robusticity. Latitudinal clines in body proportions (i.e., Allen's rule) have been well-documented in extinct and extant hominins (*Allen, 1877; Ruff, 1994; Holliday, 1997; Tilkens et al., 2007; Ruff, 2010*). Specifically, equatorial human populations, such as those from Africa, tend to have more linear body shapes and longer limbs compared to human populations from higher latitudes (e.g., the modern Chinese populations investigated in the present study), although aspects of environmental quality (e.g., nutritional differences) may modulate the phenotypic expression of these differences to some extent (*Katzmarzyk & Leonard, 1998; Bogin et al., 2002; Bogin & Varela-Silva, 2010*). This ecomorphological trend may characterize hominin body plans at least as early as archaic *H. sapiens* from the Middle Pleistocene of different regions, including East Asia (*Trinkaus et al., 1999; Ruff, 2002b; Rosenberg et al., 2006*). While a portion of the observed differences between the size-

standardized properties of Humerus II and Humerus III versus KNM-ER 1808 may be attributable to overall differences in *H. erectus* body size and limb proportions, such as would be manifested in humeral length, we attempted to control for this possibility by also incorporating estimates of body mass in these scaling factors. Thus, our estimates of comparative humeral robusticity in *H. erectus* reflect rigidity or strength *after* controlling for potential differences in estimated body size and limb length of individuals. In addition to these observed differences in humeral diaphyseal robusticity, diaphyseal shapes of Humerus II and Humerus III diverged from that of the humerus of KNM-ER 1808 (i.e., that latter exhibited comparatively more equivalent I_{max} and I_{min} values; Table 1 and Fig. 2), possibly hinting at potential differences in upper limb use. Additional suitable adult *H. erectus* humeri from both regions would be needed in order to rigorously investigate this possibility further.

Involvement of the upper limb in activities associated with selective advantages for hominins, and thus those that could be potentially worth future investigation in order to contextualize the observed differences in humeral diaphyseal robusticity, include projectile throwing (*Roach et al., 2013; Roach and Richmond, 2015*), throwing in general (*Shaw & Stock, 2009; Warden et al., 2009*), spear thrusting (*Schmitt et al., 2003*), stone tool manufacturing (*Rolian et al., 2011; Williams et al., 2012; Key & Dunmore, 2015*), and scraping (*Shaw et al., 2012*). While some (*Roach et al., 2013; Roach & Richmond, 2015*) have attributed morphological evidence of projectile throwing to *H. erectus* (e.g., low humeral torsion, an inferiorly-rotated and human-like scapula, and a tall mobile waist), there is no documented evidence of projectile use or throwing at Zhoukoudian, Locality 1. Unimanual scraping tasks, such as hide preparation, have been argued to generate bilateral asymmetry in upper limb muscle activity (*Shaw et al., 2012*), making it notable that side scrapers are the most abundant artifact in

the Locality 1 archaeological assemblage (*Pei & Zhang, 1985; Zhang, 2004; Li et al., 2011*). To date, however, experimental assessments of loading associated with stone tool use and manufacturing focus on the hand rather than the forearm or arm (*Rolian et al., 2011; Williams et al., 2012; Key & Dunmore, 2015*). The role these activities, or others, may have in inducing the dramatic right-side dominant asymmetry observed in diaphyseal strength of Late Pleistocene hominins in general (*Sládek et al., 2016; Sparacello et al., in press*), or the Late Pleistocene hominin, Tianyuan I, in particular (*Shang et al., 2007; Shang & Trinkaus, 2010*), also remain unclear. Thus, caution is warranted when assessing right and left humeri from Zhoukoudian for potential activity-related bilateral asymmetry.

While *Weidenreich (1941)* may have emphasized external surface comparisons in describing the 'thicker' Humerus II as modern human-like in its robusticity, quantitative evaluation of internal structure supports this assessment of its humeral robusticity. Evaluation of Humerus III further corroborates the suggested similarity. Despite relative cortical thicknesses of Humerus II and Humerus III (%CA) exceeding those of the majority of individuals in both modern Chinese samples investigated in the study, which themselves were characterized by comparatively robust but short humeri, comparatively expanded subperiosteal areas of the modern Chinese humeri appear to be responsible for their typically higher measures of length-standardized humeral robusticity.

In the Late Pleistocene of Southeast Asia, comparatively smaller body sizes and statures have been reported compared to contemporaneous regional populations from Africa and Europe (*Shackelford, 2007*). The comparatively short humeri of both modern Chinese samples (i.e., Datong and Junziqing) suggest that these populations also may have been relatively small-bodied, or at least that they were characterized by short humeri. Both modern Chinese samples

exhibited length-standardized humeral robusticity (e.g., sJ or sZ_p) that bracketed that of the Late Pleistocene Tianyuan 1 hominin either in the upper half (Jinziqing) or lower half (Datong) of their observed ranges. Body mass of Tianyuan 1 has been estimated as 85.1 kg (*Shang & Trinkaus, 2010*). Both modern Chinese populations also exhibited observed ranges of length-standardized humeral robusticity that broadly overlapped with those of individuals comprising the East Eurasian Late Upper Paleolithic (i.e., Minatogawa and Tam Hang). Average body mass estimates for these individuals has been estimated as 51.4 kg, with a range of 70.5 to 42.3 kg (Table 1). Assuming general equivalence or even minimal divergence in body sizes, both modern Chinese populations appear to have been characterized by less dramatic declines in humeral robusticity from Late Pleistocene levels compared to what is typically observed in Holocene populations (*Ruff et al., 1993; Trinkaus et al., 1994; Trinkaus, 1997; Ruff et al. 2015*).

There are a few constraints in the current study that bear mention. We used anatomical markers to identify diaphyseal locations in our East Asian sample (e.g., inferiormost border of deltoid insertion), as one often is resigned to relying upon when analysing fossils that do not preserve entire bone lengths. This may have resulted in a small amount of imprecision when comparing diaphyseal locations. We also had to estimate medullary cavity size and dimensions in Humerus II. While *Weidenreich (1941: Fig. 58 D)* provided information on relative size of the cavity, this was only in a single dimension so we had to assume similarity in form to Humerus III. Nonetheless, the periosteal border is more impactful on cross-sectional properties than the endosteal border, as the current study demonstrates. While we used a range of length estimates for Humerus II to standardize properties for Humerus III, reasonably similar external contours of both humeri (see Figs 1 and 2) suggest that the actual length of Humerus III probably fell within or close to this range of values. We were unable to assess the degree of bilateral asymmetry

724 expressed in Zhoukoudian *H. erectus* humeri, which is noteworthy since the left Humerus II
725 consistently exceeded the right Humerus III in structural properties. This is opposite the trend
726 typically expressed in Late Pleistocene hominins preserving both humeri (e.g., consider
727 Tianyuan 1), suggesting perhaps they represent two individuals. Finally, the observed length-
728 standardized robusticity displayed by modern Chinese samples (Datong and Junziqing) relies on
729 body size estimates not dramatically exceeding those of Late Pleistocene hominins in the region
730 (e.g., individuals from Tianyuan Cave, Minatogawa, and Tam Hang). While a broader regional
731 study of East Asian Holocene populations is beyond the scope of the current study, such a study
732 would be necessary to better understand whether the Datong and Junziqing may be
733 representative of regional trends.

734

735 **CONCLUSIONS**

736 Consistent differences were observed between the more robust humeri of East Asian *H.*
737 *erectus* (Zhoukoudian Humerus II and Humerus III) compared to the less robust humerus of
738 African *H. erectus* (KNM-ER 1808). Zhoukoudian Humerus II and Humerus III also resembled
739 Late Pleistocene hominins in humeral robusticity to a greater extent than the 1 Ma older KNM-
740 ER 1808 humerus. This indicates the presence of regional differences in *H.* erectus humeral
741 structure, which may reflect temporal trends, ecogeographic trends in body proportions, and/or
742 potential activity-related differences. Contemporaneous *H. erectus* fossils from each region could
743 begin to help resolve these non-mutually exclusive possibilities. Two modern Chinese samples
744 also exhibited increased or equivalent humeral robusticity compared to *H. erectus* (Zhoukoudian
745 Humerus II and Humerus III) and Late Pleistocene hominins from Asia (Tianyuan Cave 1,

Minatogawa, and Tam Hang). Thus, quantitative evaluation of internal humeral structure supports the original description of modern human-like robusticity of the Zhoukoudian Humerus II based on its external surface. A similar investigation of Zhoukoudian Humerus III provides corroborating support.

ACKNOWLEDGEMENTS

The authors are deeply grateful to Chris Ruff for discussions of this work, and also concerning the African *Homo erectus* humerus compared in this study. We also thank Feng Li for providing information regarding the lithic technology of Zhoukoudian *Homo erectus*. The authors also greatly appreciate assistance from Limin Zhang in preparing the CT data, and Hao Li for collecting background information on the Datong specimens.

ADDITIONAL INFORMATION AND DECLARATIONS

Funding

This work was supported by the Chinese Academy of Sciences (132311KYSB20160004) and the National Natural Science Foundation of China (4163000287, 4167020369). This work was also receive support from the Department of Science and Technology (South Africa) and the National Research Foundation (South Africa) through the African Origins Platform funding programme, as well as the Centre of Excellence in the Palaeosciences and the University of the Witwatersrand.

Grant Disclosures

Chinese Academy of Sciences (132311KYSB20160004) and the National Natural Science Foundation of China (4163000287, 4167020369)

Competing Interests

The authors declare there are no competing interests.

Author Contributions

Song Xing, Kristian J. Carlson, and Wu Liu conceived and designed the experiments; Song Xing, Kristian J. Carlson, Pianpian Wei, and Jianing He contributed to the data collection and analysis. Song Xing and Kristian J. Carlson wrote the paper.

Data Availability

The following information was supplied regarding data availability: Part of the data has been supplied as Supplementary File.

REFERENCES

Allen JA. 1877. The influence of physical conditions in the genesis of species. *Radical Review* **1**: 108-140.

Antón SC. 2002. Evolutionary significance of cranial variation in Asian *Homo erectus*. *American Journal of Physical Anthropology* **118**:301-323. DOI: 10.1002/ajpa.10091

Antón SC. 2003. The natural history of *Homo erectus*. *Yearbook of Physical Anthropology* **46**:126-170. DOI: 10.1002/ajpa.10399

Antón SC, Potts R, Aiello LC. 2014. Evolution of early *Homo*: an integrated biological perspective. *Science* **345**:1236828-1 – 1236828-13. DOI: 10.1126/science.1236828

Antón SC, Taboada HG, Middleton ER, Rainwater CW, Taylor AB, Turner TR, Turnquist JE, Weinstein KJ, Williams SA. 2016. Morphological variation in Homo erectus and the origins of developmental plasticity. *Philosophical Transactions of the Royal Society of London. Series B, Biological Science* **371**: 20150236. DOI: 10.1098/rstb.2015.0236

Baab KL. 2008. The taxonomic implications of cranial shape variation in *Homo erectus*. *Journal of Human Evolution* **54**: 827-847. https://doi.org/10.1016/j.jhevol.2007.11.003

Baba H, Narasaki S. 1991. Minatogawa Man, the oldest type of modern *H. sapiens* in East Asia. *The Quaternary Research* **30**: 221-230. http://doi.org/10.4116/jaqua.30.22

Baba H, Narasaki S, Ohyama S. 1998. Minatogawa hominid fossils and the evolution of Late Pleistocene humans in East Asia. *Anthropological Science* **106**:27-45. http://doi.org/10.1537/ase.106.Supplement_27

Binford LR, Ho CK, Aigner JS, Alimen M-H, Borrero LA, Te-K'un C, Chung T, Goldberg P, Ikawa-Smith F, Lanata JL, Zune L, Luchterhand K, Lyman RL, Goñalons GM, Pei G, Straus LG, Yacobaccio HD, Yi S. 1985. Taphonomy at a Distance: Zhoukoudian, "The cave home of Beijing Man"? *Current Anthropology* **2**: 413-442. https://doi.org/10.1086/203303

Black D. 1930. *On an adolescent skull of* Sinanthropus pekinensis *in comparison with an adult skull of the same species and with other hominid skulls, recent and fossil.* Palaeontogia Sinica Series D **7**: 1-114.

Black D. 1933. *Sinanthropus* skeletal remains, etc. In part II of "Fossil Man in China." Geolog. Memoirs, Series A No.11, pp. 63-109.

Bogin B, Smith P, Orden AB, Varela Silva MI, Loucky J. 2002. Rapid change in height and body proportions of Maya American children. *American Journal of Human Biology* **14**: 753-761.

Bogin B, Varela-Silva MI. 2010. Leg length, body proportion, and health: a review with a note on beauty. *International Journal of Environmental Research & Public Health* **7**: 1047-1075.

Carlson KJ. 2005. Investigating the form-function interface in African apes – relationships between principal moments of area and positional behaviors in femoral and humeral diaphyses. *American Journal of Physical Anthropology* **127**: 312-334. DOI: 10.1002/ajpa.20124

Carlson KJ, Grine FE, Pearson OM. 2007. Robusticity and sexual dimorphism in the postcranium of modern hunter-gatherers from Australia. *American Journal of Physical Anthropology* **134**: 9-23. DOI: 10.1002/ajpa.20617

Carlson KJ, Marchi D. (Eds). 2014. *Reconstructing mobility – environmental, behavioral, and morphological determinants*. Springer Press, New York.

Carlson KJ, Sumner DR, Morbeck ME, Nishida T, Yamanaka A, Boesch C. 2008. Role of nonbehavioral factors in adjusting long bone diaphyseal structure in free-ranging *Pan troglodytes*. *International Journal of Primatology* **29**: 1401-1420.

Chiu CL, Gu YM, Zhang YY, Chang SS. 1973. Newly discovered *Sinanthropus* remains and stone artefacts at Choukoutien. *Vertebrata Palasiatica* **11**: 109-131.

Churchill SE. 1994. *Human upper body evolution in the Eurasian Later Pleistocene*. University of New Mexico.

Crevecoeur I. 2008. Étude anthropologique du squelette du Paléolithiquesupérieur de Nazlet Khater 2 (Égypte). Leuven University Press, Leuven, Belgium (318 p.).

Davies TG, Stock JT. 2014. Human variation in the periosteal geometry of the lower limb: signatures of behaviour among human Holocene populations. In: Carlson, K.J., Marchi, D., (Eds), *Reconstructing mobility – environmental, behavioral, and morphological determinants*. Springer Press, New York. pp 67-90.

Doube M, Klosowski MM, Arganda-Carreras I, Cordeliéres F, Dougherty RP, Jackson J, Schmid B, Hutchinson JR, Shefelbine SJ. 2010. BoneJ: free and extensible bone image analysis in ImageJ. *Bone* **47**:1076-1079. https://doi.org/10.1016/j.bone.2010.08.023

Dubois E. 1894. Pithecanthropus erectus*: eine menschenähnliche Übergangsform aus Java.* Landesdruckerei, Batavia.

Dubois E. 1936. Racial identity of *Homo soloensis* Oppenoorth (including *Homo modjokertensis* von Koenigswald and *Sinanthropus pekinensis* Davidson Black). Koninklijke Akademie van Wetenschappen, *Amsterdam* **34**: 1180–1185.

Grabowski M, Hatala KG, Jungers WL, Richmond BG. 2015. Body mass estimates of hominin fossils and the evolution of human body size. *Journal of Human Evolution* **85**: 75-93. https://doi.org/10.1016/j.jhevol.2015.05.005

Howells WW. 1980. *Homo erectus* – who, when, and where: A survey. *Yearbook of Physical Anthropology* **23**: 1-23. DOI: 10.1002/ajpa.1330230503

Han W. 2005. Analyses of the racial and systematic types of residents of Beiwei Period in Datong, Shanxi Province. *Research of China's Frontier Archaeology* **4**: 270-280.

Holliday TW. 1997. Body proportions in Late Pleistocene Europe and modern human origins. *Journal of Human Evolution* **32**: 423-447. https://doi.org/10.1006/jhev.1996.0111

Hu CZ. 1973. Ape-man teeth from Yuanmou, Yunnan. *Acta Geological Sinica* **1**, 65-72.

Jacob T. 1973. Palaeoanthropological discoveries in Indonesia with special reference to the finds of the last two decades. *Journal of Human Evolution* **2**: 473-485. https://doi.org/10.1016/0047-2484(73)90125-5

Kaifu Y, Aziz F, Baba H. 2005a. Hominid mandibular remains from Sangiran: 1952-1986 Collection. *American Journal of Physical Anthropology* **128**: 497-519. DOI: 10.1002/ajpa.10427

Kaifu Y, Baba H, Aziz F, Indriati E, Schrenk F, Jacob T. 2005b. Taxonomic affinities and evolutionary history of the Early Pleistocene hominids of Java: dentognathic evidence. *American Journal of Physical Anthropology* **128**: 709-726. DOI: 10.1002/ajpa.10425

870 **Kaifu Y, Fujita M, Kono RT, Baba H. 2011.** Late Pleistocene modern human mandibles from
871 the Minatogawa Fissure site, Okinawa, Japan: morphological affinities and implications for
872 modern human dispersals in East Asia. *Anthropological Science* **119**: 137-157.
873 http://doi.org/10.1537/ase.090424

874 **Katzmarzyk PT, Leonard WR. 1998.** Climatic influences on human body size and
875 proportions: ecological adaptations and secular trends. *American Journal of Physical*
876 *Anthropology* **106**: 483-503. DOI: 10.1002/(SICI)1096-8644(199808)106:4<483::AID-
877 AJPA4>3.0.CO;2-K

878 **Key AJM, Dunmore CJ. 2015.** The evolution of the hominin thumb and the influence exerted
879 by the non-dominant hand during stone tool production. *Journal of Human Evolution* **78**: 60-
880 69. https://doi.org/10.1016/j.jhevol.2014.08.006

881 **Langbroek M, Roebroeks W. 2000.** Extraterrestrial evidence on the age of the hominids from
882 Java. *Journal of Human Evolution* **38**, 595-600.

883 **Leakey REF, Walker AC. 1985.** Further hominids from the Plio-Pleistocene of Koobi Fora,
884 Kenya. *American Journal of Physical Anthropology* **67**: 135-163.
885 DOI: 10.1002/ajpa.1330670209

886 **Li F, Wang CX, Liu DC, Zhang XL, Zhang SQ, Gao X. 2011.** Vein quartz procurement at
887 Layer 4~5 of the Zhoukoudian Locality 1. *Quaternary Science* **31**: 900-908.

888 **Liu W, Zhang Y, Wu X. 2005.** A middle Pleistocene human cranium from Tangshan, Nanjing
889 of southeast China: a comparison with *Homo erectus* from Eurasia and Africa based on new
890 reconstruction. *American Journal of Physical Anthropology* **25**: 253-262. DOI:
891 10.1002/ajpa.20066

892 **Lordkipanidze D, Jashashvili T, Vekua A, Ponce de León MS, Zollikofer CPE, Rightmire**
893 **GP, Pontzer H, Ferring R, Oms O, Tappen M, Bukhsianidze M, Agusti J, Kahlke R,**
894 **Kiladze G, Martinez-Navarro B, Mouskhelishvili A, Nioradze M, Rook L. 2007.**
895 Postcranial evidence from early *Homo* from Dmanisi, Georgia. *Nature* **449**: 305-310.
896 **Lordkipanidze D, de León MSP, Margvelashvili A, Rak Y, Rightmire GP, Vekua A,**
897 **Zollikofer CP. 2013.** A complete skull from Dmanisi, Georgia, and the evolutionary biology
898 of early *Homo*. *Science* **342**: 326-331. DOI: 10.1126/science.1238484
899 **Macintosh AA, Davies TG, Ryan TM, Shaw CN, Stock JT. 2013.** Periosteal versus true cross-
900 sectional geometry: a comparison along humeral, femoral, and tibial diaphyses. *American*
901 *Journal of Physical Anthropology* **150**: 442-452. DOI: 10.1002/ajpa.22218
902 **Matsu'ura S, Kondo M. 2011.** Relative chronology of the Minatogawa and the Upper
903 Minatogawa series of human remains from Okinawa Island, Japan. *Anthropological Science*
904 **119**: 173-182. http://doi.org/10.1537/ase.100322
905 **Mongle CS, Wallace IJ, Grine FE. 2015a.** Cross-sectional structural variation relative to
906 midshaft along hominin diaphyses. II. The forelimb. *American Journal of Physical*
907 *Anthropology* **158**: 386-397. DOI: 10.1002/ajpa.22802
908 **Mongle CS, Wallace IJ, Grine FE. 2015b.** Cross-sectional structural variation relative to
909 midshaft along hominin diaphyses. II. The hind limb. *American Journal of Physical*
910 *Anthropology* **158**: 398-407. DOI: 10.1002/ajpa.22802
911 **Mott RL. 1996.** Applied strength of materials. 3rd ed. Upper Saddle River, NJ: Prentice Hall,
912 Inc.
913 **Patole-Edoumba E, Duringer P, Richardin P, Shackelford L, Bacon A-M,**
914 **Sayavongkhamdy T, Ponche J-L, Demeter F. 2015.** Evolution of the Hoabinhian Techno-

915 Complex of Tam Hang Rockshelter in Northeastern Laos. *Archaeological Discovery* **3**:140-
916 157.
917 **Pearson OM. 2000.** Activity, climate, and postcranial robusticity. *Current Anthropology* **41**:
918 569-609. https://doi.org/10.1086/317382
919 **Pearson OM, Lieberman DE. 2004.** The aging of "Wolff's Law": ontogeny and responses to
920 mechanical loading in cortical bone. Yearbook of Physical Anthropology **47**, 63-99.
921 **Pei WZ, Zhang SS. 1985.** A study on the lithic artifacts of *Sinanthropus*. Palaeontogia Sinica
922 New Series D **12**:1-277.
923 **Polk JD, Demes B, Jungers WL, Biknevicius AR, Heinrich RE, Runestad JA. 2000.** A
924 comparison of primate, carnivoran and rodent limb bone cross-sectional properties: are
925 primates really unique? *Journal of Human Evolution* **29**: 297-325.
926 https://doi.org/10.1006/jhev.2000.0420
927 **Pontzer H, Rolian C, Rightmire GP, Jashashvili T, Ponce de León MS, Lordkipanidze D,**
928 **Zollikofer CPE. 2010.** Locomotor anatomy and biomechanics of the Dmanisi hominins.
929 *Journal of Human Evolution* **58**: 492-504. https://doi.org/10.1016/j.jhevol.2010.03.006
930 **Puymerail L, Ruff CB, Bondioli L, Widianto H, Trinkaus E, Macchiarelli R. 2012.**
931 Structural analysis of the Kresna 11 *Homo erectus* femoral shaft (Sangiran, Java). *Journal of*
932 *Human Evolution* **63**:741-749. https://doi.org/10.1016/j.jhevol.2012.08.003
933 **Rasband WS. 1997-2015.** ImageJ, U.S. National Institutes of Health, Bethesda, Maryland, USA,
934 http://imagej.nih.gov/ij/.
935 **Rightmire GP. 1993.** *The evolution of* Homo erectus. Cambridge University Press, New York.

Rightmire GP. 1998. Evidence from facial morphology for similarity of Asian and African representatives of *Homo erectus*. *American Journal of Physical Anthropology* **106**: 61-85. DOI: 10.1002/(SICI)1096-8644(199805)106:1<61::AID-AJPA5>3.0.CO;2-G

Roach NT, Venkadesan M, Rainbow MJ, Lieberman DE. 2013. Elastic energy storage in the shoulder and the evolution of high-speed throwing in *Homo*. *Nature* **498**: 483-487. DOI:10.1038/nature12267

Roach NT, Richmond BG. 2015. Clavicle length, throwing performance and the reconstruction of the *Homo erectus* shoulder. *Journal of Human Evolution* **80**: 107-113. https://doi.org/10.1016/j.jhevol.2014.09.004

Rolian C, Lieberman DE, Zermeno JP. 2011. Hand biomechanics during simulated stone tool use. *Journal of Human Evolution* **61**: 26-41. https://doi.org/10.1016/j.jhevol.2011.01.008

Rosenberg KR, Lü Z, Ruff CB. 2006. Body size, body proportions and encephalization in a Middle Pleistocene archaic human from northern China. DOI: 10.1073/pnas.0508681103*Proceedings of the National Academy of Sciences of the United States of America* **103**: 3552-3556.

Ruff CB. 1994. Morphological adaptation to climate in modern and fossil hominids. *Yearbook of Physical Anthropology* **37**: 65-107. DOI: 10.1002/ajpa.1330370605

Ruff CB. 2000. Body size, body shape, and long bone strength in modern humans. *Journal of Human Evolution* **38**: 269-290. https://doi.org/10.1006/jhev.1999.0322

Ruff CB. 2002a. Long bone articular and diaphyseal structure in Old World monkeys and apes. I: locomotor effects. *American Journal of Physical Anthropology* **119**: 305-342. DOI: 10.1002/ajpa.10117

Ruff CB. 2002b. Variation in human body size and shape. *Annual Review of Anthropology* **31**: 211-232. https://doi.org/10.1146/annurev.anthro.31.040402.085407

Ruff CB. 2003a. Growth in bone strength, body size, and muscle size in a juvenile longitudinal sample. *Bone* **33**: 317-329. https://doi.org/10.1016/S8756-3282(03)00161-3

Ruff CB. 2003b. Ontogenetic adaptation to bipedalism: age changes in femoral to humeral length and strength proportions in humans, with a comparison to baboons. *Journal of Human Evolution* **45**: 317-349. https://doi.org/10.1016/j.jhevol.2003.08.006

Ruff CB. 2008. Femoral/humeral strength in early African *Homo erectus*. *Journal of Human Evolution* **54**:383-390. https://doi.org/10.1016/j.jhevol.2007.09.001

Ruff CB. 2009. Relative limb strength and locomotion in *Homo habilis*. *American Journal of Physical Anthropology* **138**: 90-100. DOI: 10.1002/ajpa.20907

Ruff CB. 2010. Body size and body shape in early hominins – implications of the Gona pelvis. *Journal of Human Evolution* **58**: 166-178. https://doi.org/10.1016/j.jhevol.2009.10.003

Ruff CB, Puymerail L, Macchiarelli R, Sipla J, Ciochon RL. 2015. Structure and composition of the Trinil femora: functional and taxonomic implications. *Journal of Human Evolution* **80**:147-158. https://doi.org/10.1016/j.jhevol.2014.12.004

974 **Ruff CB., Holt B, Niskanen M, Sladek V, Berner M, Garofalo E, Garvin HM, Hora M,**
975 **Junno J-A, Schuplerova E, Vilkama R, Whitney E. 2015.** Gradual decline in mobility with
976 the adoption of food production in Europe. *Proceedings of the National Academy of Sciences*
977 *of the United States of America* **112**: 7147-7152. DOI: 10.1073/pnas.1502932112

978 **Ruff CB, Holt B, Trinkaus E. 2006.** Who's afraid of the big bad Wolff?: Wolff's Law" and
979 bone functional adaptation. *American Journal of Physical Anthropology* **129**: 484-498. DOI:
980 10.1002/ajpa.20371

981 **Ruff CB, Larsen CS. 2014.** Long bone structural analyses and the reconstruction of past
982 mobility: a historical review. In: Carlson, K.J., Marchi, D., (Eds), *Reconstructing mobility –*
983 *environmental, behavioral, and morphological determinants*. Springer Press, New York. pp
984 13-30.

985 **Ruff CB, Trinkaus E, Walker A, Larsen CS. 1993.** Postcranial robusticity in *Homo*. I:
986 Temporal trends and mechanical interpretation. *American Journal of Physical Anthropology*
987 **91**: 21-53. DOI: 10.1002/ajpa.1330910103

988 **Ruff CB, Walker A. 1993.** Body size and body shape. In: Walker, A., Leakey, R. (Eds.). *The*
989 *Nariokotome Homo erectus skeleton*. Harvard University Press, Cambridge, pp. 234-265.

990 **Santa Luca AP. 1980.** *The Ngandong fossil hominids*. Department of Anthropology, Yale
991 University, New Haven.

992 **Schmitt D, Churchill SE, Hylander WL. 2003.** Experimental evidence concerning spear use in
993 Neanderthals and early modern humans. *Journal of Archaeological Science* **30**: 103-114.
994 https://doi.org/10.1006/jasc.2001.0814

995 **Shackelford LL. 2007.** Regional variation in the postcranial robusticity of Late Upper
996 Paleolithic humans. *American Journal of Physical Anthropology* **133**: 655-668. DOI:
997 10.1002/ajpa.20567

998 **Shackelford LL, Demeter F. 2012.** The place of Tam Hang in Southeast Asian human
999 evolution. *Comptes Rendus Palevol* **11**: 97-115. https://doi.org/10.1016/j.crpv.2011.07.002

1000 **Shang H, Tong H, Zhang S, Chen F, Trinkaus E. 2007.** An early modern human from
1001 Tianyuan Cave, Zhoukoudian, China. *Proceedings of the National Academy of Sciences of the*
1002 *United States of America* **104**: 6573-5678. DOI: 10.1073/pnas.0702169104

1003 **Shang H, Trinkaus E. 2010.** *The early modern human from Tianyuan Cave, China*. Texas
1004 A&M University Press, College Station, TX.

1005 **Shaw CN, Hofmann CL, Petraglia MD, Stock JT, Gottschall JS. 2012.** Neanderthal humeri
1006 may reflect adaptation to scraping tasks, but not spear thrusting. *PLoS One* **7**: e40349.
1007 https://doi.org/10.1371/journal.pone.0040349

1008 **Shaw CN, Stock JT. 2009.** Habitual throwing and swimming correspond with upper limb
1009 diaphyseal strength and shape in modern human athletes. *American Journal of Physical*
1010 *Anthropology* **140**: 160-172. DOI: 10.1002/ajpa.21063

1011 **Shaw CN, Stock JT, Davies TG, Ryan TM. 2014.** Does the distribution and variation in
1012 cortical bone along the lower limb diaphyses reflect selection for locomotor economy. In:
1013 Carlson, K.J., Marchi, D., (Eds), *Reconstructing mobility – environmental, behavioral, and*
1014 *morphological determinants*. Springer Press, New York. pp 49-66.

1015 **Shen G, Gao X, Gao B, Granger DE. 2009.** Age of Zhoukoudian *Homo erectus* determined
1016 with $^{26}Al/^{10}Be$ burial dating. *Nature* **458**: 198-200.

1017 **Sládek V, Berner M, Galeta P, Friedl L, Kudrnová Š. 2010.** Technical note: the effect of
1018 midshaft location on the error ranges of femoral and tibial cross-sectional parameters.
1019 *American Journal of Physical Anthropology* **141**: 325-332. DOI: 10.1002/ajpa.21153

1020 **Sládek V, Ruff CB, Berner M, Holt B, Niskanen M, Schuplerová E, Hora M. 2016.** The
1021 impact of subsistence changes on humeral bilateral asymmetry in Terminal Pleistocene and
1022 Holocene Europe. *Journal of Human Evolution* **92**: 37-49.
1023 https://doi.org/10.1016/j.jhevol.2015.12.001

1024 **Sparacello VS, Villotte S, Shackelford LL. Trinkaus E. 2016.** Patterns of humeral asymmetry
1025 among Late Pleistocene humans. *Comptes Rendus Palevol*
1026 http://dx.doi.org/10.1016/j.crpv.2016.09.001.

1027 **Stock JT. 2006.** Hunter-gatherer postcranial robusticity relative to patterns of mobility, climatic
1028 adaptation and selection for tissue economy. *American Journal of Physical Anthropology* **131**:
1029 194-204. DOI: 10.1002/ajpa.20398

1030 **Stock JT, Shaw CN. 2007.** Which measures of diaphyseal robusticity are robust? A comparison
1031 of external methods of quantifying the strength of long bone diaphysis to cross-sectional
1032 geometric properties. *American Journal of Physical Anthropology* **134**: 412-423. DOI:
1033 10.1002/ajpa.20686

1034 **Stringer CB. 1984.** The definition of *Homo erectus* and the existence of the species in Africa
1035 and Europe. *Courier Forschungsinstitut Senckenberg* **9**: 131-143.

1036 **Swisher CC III, Curtis GH, Jacob T, Getty AG, Widiasmoro AS. 1994.** Age of the earliest
1037 known hominids in Java, Indonesia. *Science* **263**:118–1121.

1038 **Swisher CC III, Rink WJ, Antón SC, Schwarcz HP, Curtis GH, Widiasmoro AS. 1996.**
1039 Latest *Homo erectus*, in Java: potential contemporaneity with *Homo sapiens* in Southeast
1040 Asia. *Science* **274**: 1870-1874.

1041 **Tilkens MJ, Wall-Scheffler C, Weave TD, Steudel-Numbers K. 2007.** The effects of body
1042 proportions on thermoregulation: an experimental assessment of Allen's rule. *Journal of*
1043 *Human Evolution* **53**: 286-291. https://doi.org/10.1016/j.jhevol.2007.04.005

1044 **Tong H, Shang H, Zhang S, Chen F. 2004.** A preliminary report on the newly found Tianyuan
1045 Cave, a Late Pleistocene human fossil site near Zhoukoudian. *Chinese Science Bulletin* **49**:
1046 853-857.

1047 **Trinkaus E. 1997.** Appendicular robusticity and the paleobiology of modern human emergence.
1048 *Proceedings of the National Academy of Sciences of the United States of America* **94**: 13367-
1049 13373.

1050 **Trinkaus E, Churchill SE, 1999.** Diaphyseal cross-sectional geometry of Near Eastern Middle
1051 Palaeolithic humans: the humerus. *Journal of Archaeological Science* **26**: 173–184.
1052 https://doi.org/10.1006/jasc.1998.0314

1053 **Trinkaus E, Churchill SE, Ruff CB. 1994.** Postcranial robusticity in *Homo*. II: humeral
1054 bilateral asymmetry and bone plasticity. *American Journal of Physical Anthropology* **93**: 1-
1055 34. DOI: 10.1002/ajpa.1330930102

1056 **Trinkaus E, Stringer CB, Ruff CB, Hennessy RJ, Roberts MB, Parfitt SA.**

1057 **1999.** Diaphyseal cross-sectional geometry of the Boxgrove 1 Middle Pleistocene human
1058 tibia. *Journal of Human Evolution* **37**: 1-25. https://doi.org/10.1006/jhev.1999.0295

Ungar PS, Grine FE, Teaford MF. 2006. Diet in early *Homo*: a review of the evidence and a new model of adaptive versatility. *Annual Review of Anthropology* **35**: 209-228.

Von Koenigswald GHR. 1936. Ein fossiler Hominide aus dem Altpleistocän Ostjavas. De Ingenieur in Ned.-Indië, Mijnbouw & Geologie, De Mijningenieur **4**: 149-157.

Von Koenigswald GHR. 1940. Neue *Pithecanthropus* – Funde 1936-38, Eine Beitrag zur Kenntnis der Praehominiden. Diens Mijnbow Ned. Indie, We. Meded. 28 Landsdrukkerij, pp. 1 – 205.

Von Koenigswald GHR. 1951. Introduction. In: Weidenreich, F., *Morphology of Solo Man*. Anthropol. Pap. Am. Mus. Nat. Hist. 43, part 3, 211-221.

Wallace IJ, Tommasini SM, Judex S, Garland Jr T, Demes B. 2012. Genetic variations and physical activity as determinants of limb bone morphology: An experimental approach using a mouse model. *American Journal of Physical Anthropology* **148**:24-35. **DOI:** 10.1002/ajpa.22028

Walker A, Leakey RE. 1993. The Nariokotome *Homo erectus* skeleton. Springer, Netherlands.

Walker A, Zimmerman MR, Leakey REF. 1982. A possible case of hypervitaminosis A in *Homo erectus*. *Nature* **296**: 248-250.

Warden SJ, Bogenschutz ED, Smith HD, Gutierrez AR. 2009. Throwing induces substantial torsional adaptation within the midshaft humerus of male baseball players. *Bone* **45**: 931-941. https://doi.org/10.1016/j.bone.2009.07.075

Weidenreich F. 1938. Discovery of the femur and the humerus of *Sinanthropus pekinensis*. *Nature* **141**: 614-617. DOI:10.1038/141614a0

Weidenreich F. 1941. *The extremity bones of* Sinanthropus pekinensis*,* Palaeontogia Sinica New Series D 5.

Weidenreich F. 1943. *The skull of* Sinanthropus pekinenesis*: a comparative study on a primitive hominid skull*. Palaeontogia Sinica New Series D **10**: 1-298.

Weiner S, Xu Q, Goldberg P, Liu J, Bar-Yosef O. 1998. Evidence for the use of fire at Zhoukoudian, China. *Science* **281**: 251-253. DOI: 10.1126/science.281.5374.25

Will M, Stock JT. 2015. Spatial and temporal variation of body size among early *Homo*. *Journal of Human Evolution* **82**: 15-33. https://doi.org/10.1016/j.jhevol.2015.02.009

Williams EM, Gordon AD, Richmond BG. 2012. Hand pressure distribution during Oldowan stone tool production. *Journal of Human Evolution* **62**: 520-532. https://doi.org/10.1016/j.jhevol.2012.02.005

Woo J-K. 1964. Mandible of *Sinanthropus lantianensis*. *Current Anthropology* 5, 98-101. https://doi.org/10.1086/200457

Woo J-K. 1966. The skull of Lantian Man. Current Anthropology **7**: 83-86. https://doi.org/10.1086/200664

Woo J, Chia L. 1954. New discoveries of *Sinanthropus pekinensis* in Choukoutien. *Acta Palaeontologica Sinica* **2**: 267-288.

Wood B. 1994. Taxonomy and evolutionary relationships of *Homo erectus*. *Courier Forschungsinstitut Senckenberg* **171**:159-165.

Wu R, Dong X. 1982. Preliminary study of *Homo erectus* from Hexian, Anhui. *Acta Anthropologica Sinica* **1**: 2-13.

Wu X. 1999. Investigating the possible use of fire at Zhoukoudian, China. *Science* **283**: 299. DOI: 10.1126/science.283.5400.299a

Wu X, Poirier FE. 1995. *Human evolution in China*. Oxford University Press, Oxford.

Xie Y, Xing H, Xu J, Zhou B, Huang Y, Liu Y, Qu Z. 1985. The sedimentary environment of the Peking Man period. *Multidisciplinary study of the Peking Man site at Zhoukoudian*. Science Press, Beijing, pp.185-215.

Zaim Y, Ciochon RL, Polanski JM, Grine FE, Bettis EA III, Rizal Y, Franciscus RG, Larick RR, Heizler M, Aswan Eaves KL, Marsh HE. 2011. New 1.5 million-year-old *Homo erectus* maxilla from Sangiran (Central Java, Indonesia). *Journal of Human Evolution* **61**: 363-376. https://doi.org/10.1016/j.jhevol.2011.04.009

Zhang GW, Hu YW, Pei DM, Song GD, Wang CS. 2010. Stable isotope analysis of human skeletons from the Datong Beiwei archaeological site (southern suburbs). *Cultural relics in Southern China* **1**: 127-131.

Zhang SS. 2004. *Beijing Annals: world Cultural Heritage Volume – the Peking Man Ruins Annals*. Beijing Press, Beijing.

Zhang Y, Tang ZW. 2007. Discussion of the paleoenvironment of the Peking Man site. *Acta Anthropologica Sinica* **26**: 34-44.

Zhu RX, Potts R, Pan YX, Yao HT, Lü LQ, Zhao X, Gao X, Chen LW, Gao F, Deng CL. 2008. Early evidence of the genus *Homo* in East Asia. *Journal of Human Evolution* **55**: 1075-1085. https://doi.org/10.1016/j.jhevol.2008.08.005

FIGURE CAPTIONS

Figure 1. Zhoukoudian partial right humerus (PA64, Humerus III). Standard anatomical views of the fossil (scale 1cm). On the far right, a rendering (yellow) created from Humerus III is superimposed on a mirrored rendering (light blue) created from the composite cast of Humerus II. Note general correspondence in external shape and morphology between the midshaft regions of Humerus II and Humerus III renderings. Weidenreich (1941) estimated maximum length of the Humerus II rendering as 324.0 mm.

Figure 2. Humeral cross sections. In the upper three rows, midshaft cross sections are illustrated for Zhoukoudian Humerus II and Humerus III, Tianyuan 1 right and left humeri, and Datong humeri (n = 10). The reconstructed cross section from the left humerus of Tianyuan 1 has missing cortical bone estimated in green. In the bottom row, cross sections are illustrated for a second, more distal location of Zhoukoudian Humerus II and Humerus III. Both estimated cross sections from the Weidenreich composite cast of Humerus II have been mirrored for illustration purposes. All midshaft cross sections from the Junziqing humeri (n = 23) are illustrated in Figure S2.

Figure 3. Box plots of percent cortical area (%CA) in humeral midshaft cross sections. Solid horizontal lines within boxes indicate median values, while height of boxes indicates interquartile range (i.e., contains 50% of observations) and whiskers indicate the observed highest and lowest values that do not exceed 1.5 times the interquartile range. Note that the cross section for KNM-ER 1808 is an estimated 40% diaphyseal length rather than midshaft (Ruff, 2008).

Figure 4. Box plots of standardized polar section modulus (Z_p) from the humeral midshaft. Data and standardization procedures are reported in the methods section (see also Tables 4 and 5). The three different horizontal lines illustrated for Zhoukoudian Humerus II and Humerus III indicate the three different maximum lengths used to standardize their raw values.

Figure 1

Figure 1

Figure 1. Zhoukoudian partial right humerus (PA64, Humerus III). Standard anatomical views of the fossil (scale 1cm). On the far right, a rendering (yellow) created from Humerus III is superimposed on a mirrored rendering (light blue) created from the composite cast of Humerus II. Note general correspondence in external shape and morphology between the midshaft regions of Humerus II and Humerus III renderings. *Weidenreich (1941)* estimated maximum length of the Humerus II rendering as 324.0 mm.

**Note: Auto Gamma Correction was used for the image. This only affects the reviewing manuscript. See original source image if needed for review.*

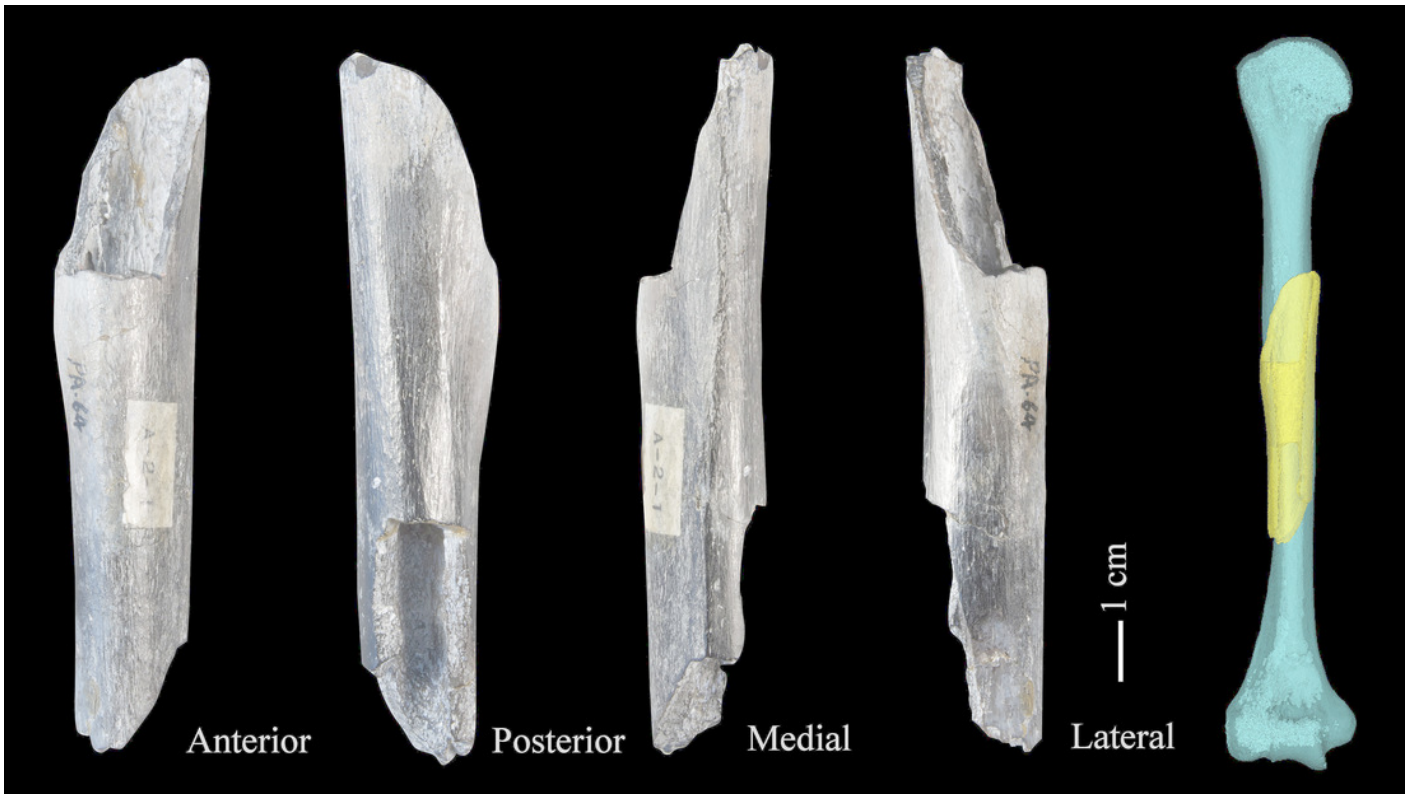

Figure 2

Figure 2

Figure 2. Humeral cross sections. In the upper three rows, midshaft cross sections are illustrated for Zhoukoudian Humerus II and Humerus III, Tianyuan 1 right and left humeri, and Datong humeri (n = 10). The reconstructed cross section from the left humerus of Tianyuan 1 has missing cortical bone estimated in green. In the bottom row, cross sections are illustrated for a second, more distal location of Zhoukoudian Humerus II and Humerus III. Both estimated cross sections from the Weidenreich composite cast of Humerus II have been mirrored for illustration purposes. All midshaft cross sections from the Junziqing humeri (n = 23) are illustrated in Figure S2.

**Note: Auto Gamma Correction was used for the image. This only affects the reviewing manuscript. See original source image if needed for review.*

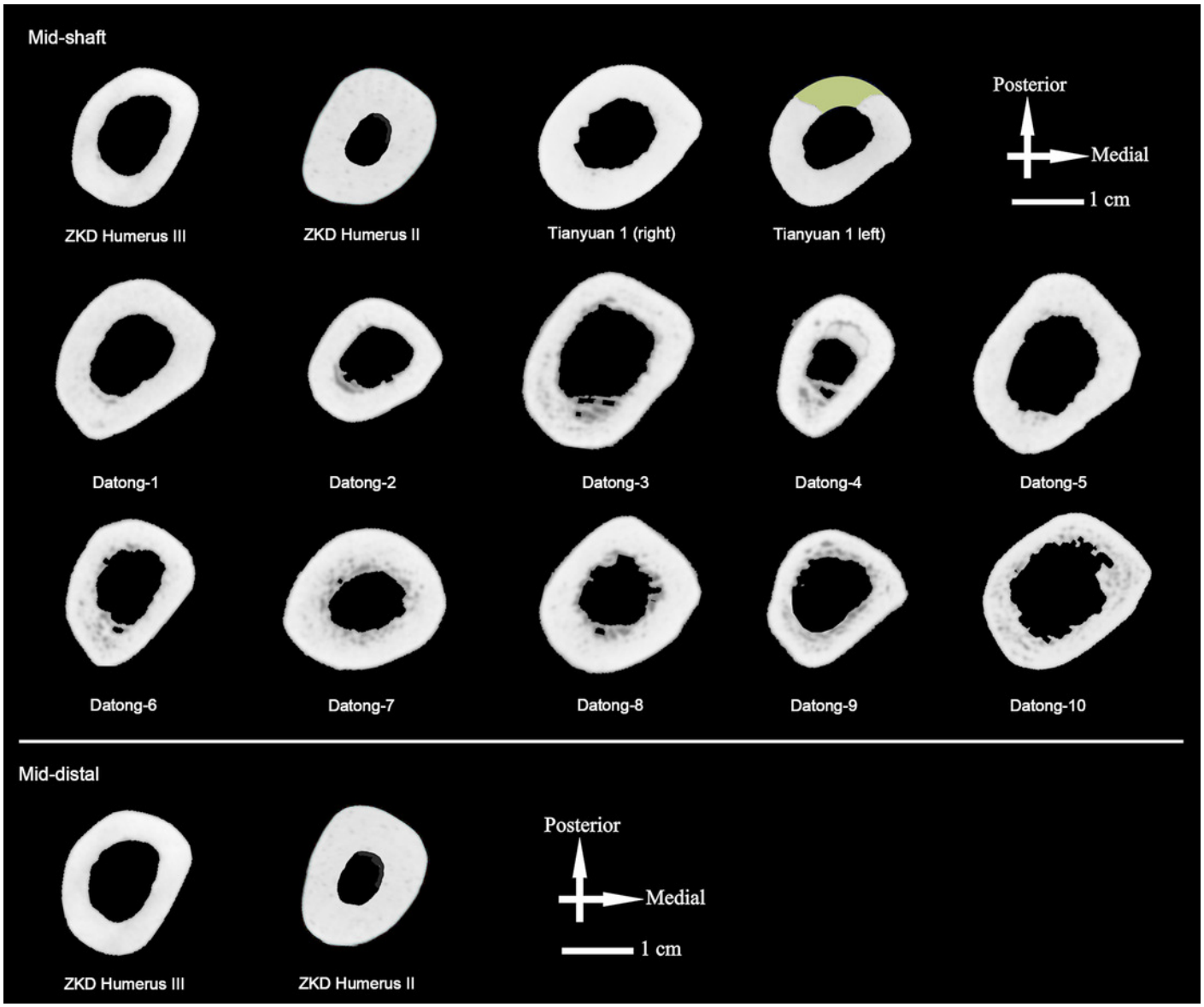
Mid-shaft
Posterior
Medial
1 cm
ZKD Humerus III
ZKD Humerus II
Tianyuan 1 (right)
Tianyuan 1 left)
Datong-1
Datong-2
Datong-3
Datong-4
Datong-5
Datong-6
Datong-7
Datong-8
Datong-9
Datong-10
Mid-distal
Posterior
Medial
1 cm
ZKD Humerus III
ZKD Humerus II

Figure 3(on next page)

Figure 3

Figure 3. Box plots of percent cortical area (%CA) in humeral midshaft cross sections. Solid horizontal lines within boxes indicate median values, while height of boxes indicates interquartile range (i.e., contains 50% of observations) and whiskers indicate the observed highest and lowest values that do not exceed 1.5 times the interquartile range. Note that the cross section for KNM-ER 1808 is an estimated 40% diaphyseal length rather than midshaft *(Ruff, 2008)*.

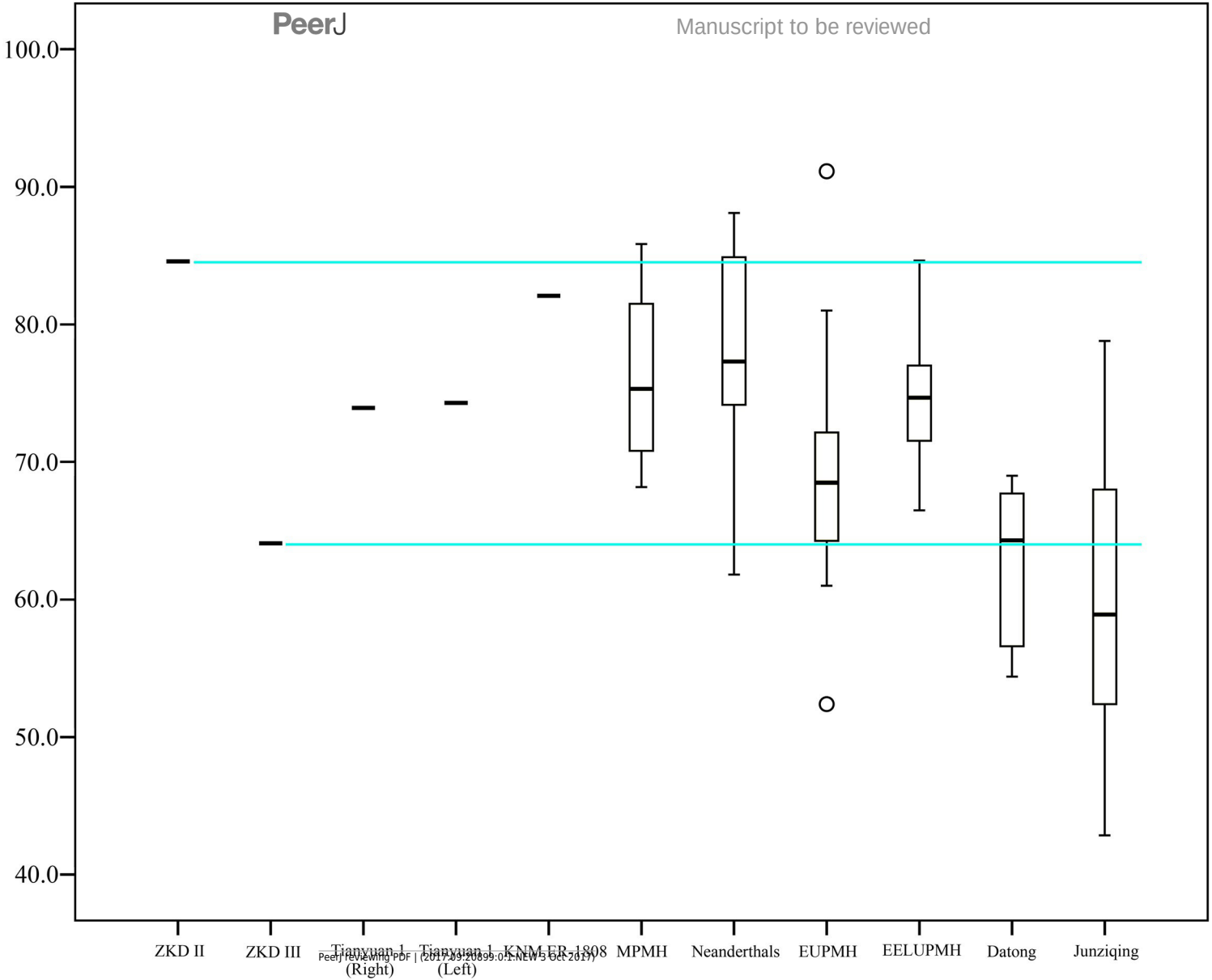
100.0
90.0
80.0
70.0
60.0
50.0
40.0
ZKD II
ZKD III
Tianyuan 1 (Right)
Tianyuan 1 (Left)
KNM ER 1808
MPMH
Neanderthals
EUPMH
EELUPMH
Datong
Junziqing

Figure 4(on next page)

Figure 4

Figure 4. Box plots of standardized polar section modulus (Z_p) from the humeral midshaft. Data and standardization procedures are reported in the methods section (see also Tables 4 and 5). The three different horizontal lines illustrated for Zhoukoudian Humerus II and Humerus III indicate the three different maximum lengths used to standardize their raw values.

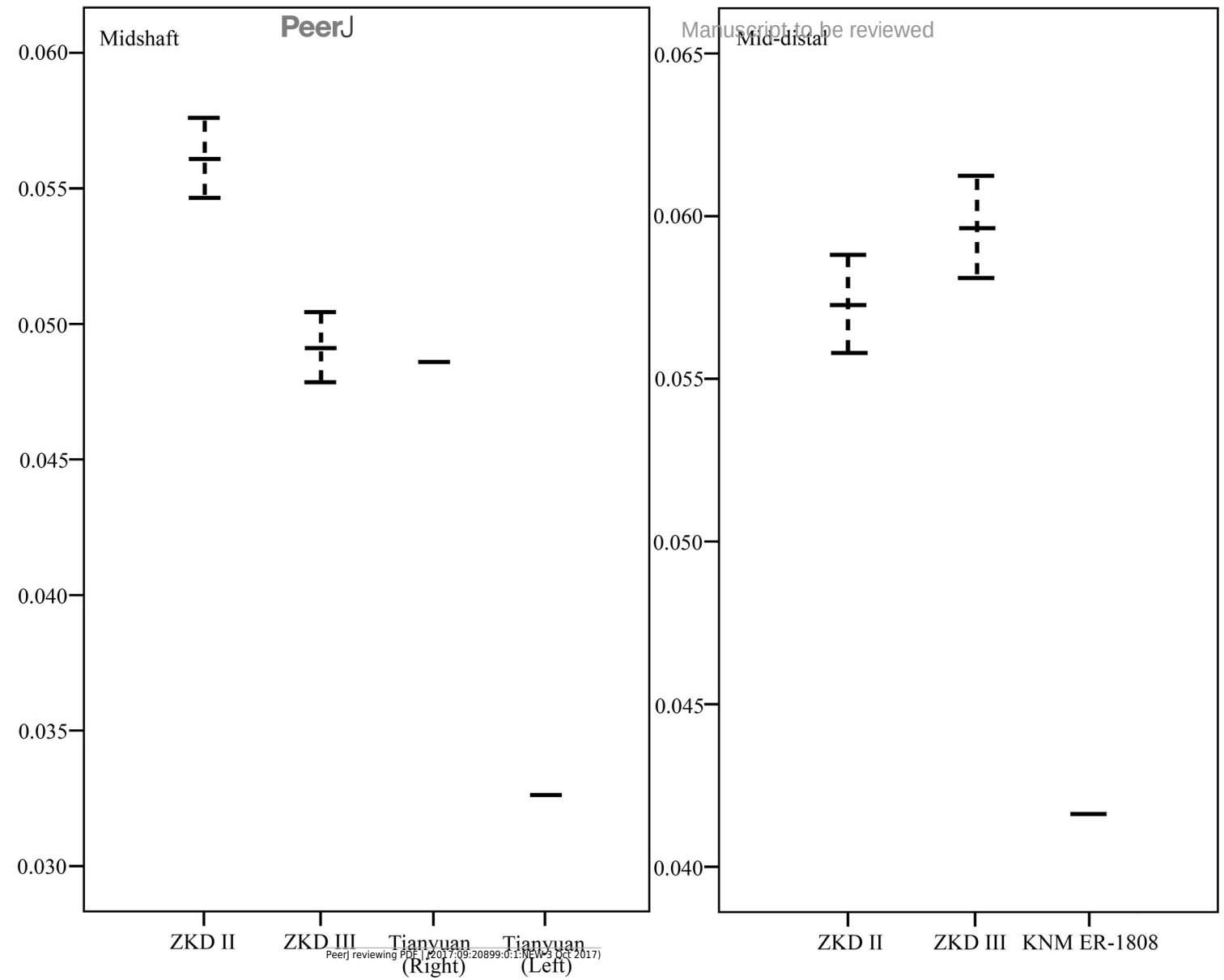

Table 1(on next page)

Table 1

Table 1. Midshaft humeral unstandardized properties of Zhoukoudian right humerus (III) and comparative samples.

Table 1. Midshaft humeral unstandardized properties of Zhoukoudian right humerus (III) and comparative samples.

		Length (mm)	Body Mass (kg)	TA (mm^2)	CA (mm^2)	%CA	I_{max} (mm^4)	I_{min} (mm^4)	Z_{max} (mm^3)	Z_{min} (mm^3)	J (mm^4)	Z_p (mm^3)
Zhoukoudian III*[1]		307.4- 324.0	53.6	250	167	66.8	5959	3307	579	415	9266	875
KNM-ER 1808[2]		350.0	60.2	240	197	82.1	5212	3891	503	457	9103	877
Tianyuan 1*[3]		327.4	85.1	330	249	75.5	10561	6345	912	684	16906	1391
Middle Paleolithic Modern Human[4]	Mean	358.3	66.1	303.5	235.3	76.2	8152	5216	-	-	13368	-
(n=4 for length, TA, CA, I_x, and I_y, n=2	S.D.	20.5	3.9	80.5	81.3	7.4	4452	2985	-	-	7395	-
for body mass, n=5 for I_{max}, I_{min}, and J)	Min	329.0	63.3	190.7	130.0	68.2	3591	1946	-	-	5537	-
	Max	375.0	68.8	381.4	327.4	85.8	14567	8834	-	-	23401	-
Neanderthals[4]	Mean	301.6	71.5	314.8	244.5	77.8	9373	5444	-	-	14945	-
(n=12 for length, n=9 for body mass, n=12	S.D.	20.6	10.1	79.3	65.6	7.7	4062	2479	-	-	6246	-
for TA, CA, I_x, and I_y, n=14 for I_{max} and	Min	262.0	59.9	183.3	125.3	61.8	3705	1887	-	-	5592	-
I_{min}, n=15 for J)	Max	335.5	85.5	426.0	365.9	88.1	14787	9757	-	-	24544	-
Early Upper Paleolithic Modern	Mean	332.6	69.0	330.7	227.4	69.6	9317	6094	-	-	15411	-
Human[4] (n=17 for length, n=13 for body	S.D.	25.9	7.8	73.4	48.6	9.2	3558	2253	-	-	5716	-
mass, n=14 for TA, CA, I_x, and I_y, n=22	Min	284.0	55.7	181.5	143.0	52.4	3210	2207	-	-	5417	-
for I_{max}, I_{min}, and J)	Max	371.0	82.5	444.2	316.8	91.1	17592	10579	-	-	27736	-
East Eurasia Late Upper Paleolithic[4]	Mean	274.3	51.4	232.1	172.5	74.7	5612	2937	-	-	8549	
(n=9 for length, n=8 for body mass, n=10	S.D.	18.1	9.9	30.5	18.7	5.1	1570	774	-	-	2251	
for TA, CA, I_x, I_y, I_{max}, I_{min}, and J)	Min	252.0	42.3	189.5	153.6	66.5	3671	2132	-	-	5803	
	Max	311.0	70.5	283.1	218.0	84.6	8331	4486	-	-	12817	
Datong (n=10)[5]	Mean	305.8	-	308	193	62.8	8660	5360	742	548	14020	1143
	S.D.	18.2	-	69	46	5.7	3743	2254	251	196	5951	395
	Min	272.4	-	210	131	54.4	4134	2166	401	307	6336	601
	Max	328.0	-	397	258	69.0	14107	8751	1072	831	22858	1715
Junziqing (n=23)[5]	Mean	286.2	-	268	161	59.7	6199	3958	565	451	10157	915
	S.D.	17.5	-	50	44	10.8	2514	1663	190	143	4132	308
	Min	262.9	-	193	90	42.9	2678	1722	288	255	4632	497
	Max	327.7	-	384	243	78.8	11814	7540	988	738	18877	1571

*Estimated cross section location due to incomplete length. [1]The maximum length of the left Zhoukoudian Humerus II was reported by *Weidenreich (1941)* to be 324.0 mm. We estimated maximum length as 307.4 mm using a regression analysis of the distance between the deltoid tuberosity and the proximal margin of the olecranon fossa against maximum length on our comparative sample of Datong and Qing modern *Homo sapiens* (n = 33; see Text S1). In order to be conservative, we use both estimates to provide a range of standardized values for Zhoukoudian humeri about a mean value (315.7 mm). In order to standardize cross-sectional properties, we used maximum length estimates of the reconstructed left Zhoukoudian Humerus II as proxies for maximum length estimates of the partial right Zhoukoudian Humerus III. [2]Cross-sectional data for a 40% length section published by *Ruff (2008)*. We used a rough approximation of 350.0 mm for humeral length (*Ruff, 2008; pers. comm*). [3]In order to standardize cross-sectional properties, but acknowledging substantial bilateral asymmetry in their cross-sectional properties, we chose to use biomechanical length of the left Tianyuan 1 humerus (327.4 mm: *Shang & Trinkaus, 2010*) as a proxy for length of the right Tianyuan 1 humerus. [4]Data from *Churchill (1994)*, *Trinkaus et al. (1994)*, *Trinkaus & Churchill (1999)*, *Crevecoeur (2008)*, and *Sparacello et al. (2016)*. [5]Amongst the recent modern human comparative sample, the inferiormost point of the deltoid tuberosity was between 43 and 53% shaft length, with the majority of specimens falling between 46 and 51%.

Table 2(on next page)

Table 2

Table 2. Midshaft humeral unstandardized properties of Zhoukoudian left humerus (II) and comparative samples.

Table 2. Midshaft humeral unstandardized properties of Zhoukoudian left humerus (II) and comparative samples.

		Length (mm)	Body mass (kg)	TA (mm^2)	CA (mm^2)	%CA	I_{max} (mm^4)	I_{min} (mm^4)	Z_{max} (mm^3)	Z_{min} (mm^3)	J (mm^4)	Z_p (mm^3)
Zhoukoudian II*[1]		307.4-324.0	53.6	261	228	87.4	6985	4143	640	518	11128	1009
Tianyuan 1*[2]		327.4	85.1	252	190	75.4	5931	3868	603	463	9799	928
Middle Paleolithic Modern Human[3] (n=2 for length, body mass, TA, CA, I_x, and I_y, n=3 for I_{max}, I_{min}, and J)	Mean	353.3	68.9	283.1	217.0	76.8	5894	4088	-	-	9981	-
	S.D.	30.8	0.1	5.2	56.9	21.5	2021	1619	-	-	3618	-
	Min	331.5	68.8	279.4	176.7	61.6	3564	2287	-	-	5851	-
	Max	375.0	69.0	286.7	257.2	92.1	7170	5421	-	-	12591	-
Neanderthals[3] (n=5 for length, n=4 for body mass, n=7 for TA and CA, n=6 for I_x and I_y, n=8 for I_{max} and I_{min}, n=9 for J)	Mean	314.4	79.1	256.0	197.8	77.6	7879	4173	-	-	12112	-
	S.D.	13.4	9.7	44.0	29.3	3.6	2863	1658	-	-	4199	-
	Min	299	64.8	203.5	170.7	73.9	4629	2250	-	-	6879	-
	Max	334	85.5	341.1	251.9	84.2	12020	6411	-	-	18250	-
Early Upper Paleolithic Modern Human[3] (n=20 for length, n=15 for body mass, n=17 for TA, CA, I_x, and I_y, n=22 for I_{max} and I_{min}, n=23 for J)	Mean	326.5	68.4	298.6	198.6	67.1	7119	4799	-	-	12138	-
	S.D.	21.0	7.7	46.1	29.5	8.9	1965	1315	-	-	2978	-
	Min	288.0	54.3	199.8	133.0	47.9	3670	2148	-	-	5895	-
	Max	370.0	82.5	394.1	246.7	83.0	10701	7316	-	-	17605	-
East Eurasia Late Upper Paleolithic[3] (n=7 for length, n=5 for body mass, n=10 for TA, CA, I_x, I_y, I_{max}, I_{min}, and J)	Mean	273.1	53.2	227.6	168.4	74.2	5106	2972	-	-	8078	-
	S.D.	20.3	10.5	33.8	27.9	7.6	1463	955	-	-	2395	-
	Min	250.0	42.3	186.7	138.8	65.7	3437	1900	-	-	5587	-
	Max	311.0	70.5	281.8	225.1	86.5	7432	4724	-	-	11968	-

*Estimated cross section location due to incomplete length. [1] The maximum length of the left Zhoukoudian Humerus II was reported by *Weidenreich (1941)* to be 324.0 mm. We estimated maximum length as 307.4 mm using a regression analysis of the distance between the deltoid tuberosity and the proximal margin of the olecranon fossa against maximum length on our comparative sample of Datong and Qing modern *Homo*

sapiens (n = 33; see Text S1). In order to be conservative, we use both estimates to provide a range of standardized values for Zhoukoudian humeri about a mean value (315.7 mm). We estimated cross-sectional properties of Humerus II from its periosteal contour, which are generally comparable to cross-sectional properties calculated from cross sections with medullary cavities (*Macintosh et al., 2013*), although some caution is warranted when percentage cortical area is known to vary dramatically. [2]Data from *Shang &Trinkaus (2010)*. [3]Data from *Churchill (1994)*, *Trinkaus et al. (1994)*, *Trinkaus & Churchill (1999)*, *Crevecoeur (2008)*, and *Sparacello et al. (2016)*.

Table 3(on next page)

Table 3

Table 3. Midshaft humeral standardized properties (by estimated body mass x maximum length) of Zhoukoudian right humerus (III) and comparative samples*.

Table 3. Midshaft humeral standardized properties (by estimated body mass x maximum length) of Zhoukoudian right humerus (III) and comparative samples*.

		sI_{max}	sI_{min}	sZ_{max}	sZ_{min}	sJ	sZ_p
ZKD Humerus III	(307.4)	0.362	0.201	0.035	0.025	0.562	0.053
	(315.7)	0.352	0.195	0.034	0.0245	0.548	0.052
	(324.0)	0.343	0.190	0.033	0.024	0.534	0.050
KNM-ER 1808		0.247	0.185	0.024	0.022	0.432	0.042
Tianyuan 1		0.379	0.228	0.033	0.025	0.607	0.050
Middle Paleolithic Modern Human (n=2)	Mean	0.339	0.282	-	-	0.682	-
	S.D.	0.099	0.047	-	-	0.146	-
	Min	0.329	0.249	-	-	0.579	-
	Max	0.469	0.315	-	-	0.785	-
Neanderthals (n=8 for sTA, sCA, sImax, and sImin, n=9 for sJ)	Mean	0.420	0.244	-	-	0.682	-
	S.D.	0.165	0.117	-	-	0.265	-
	Min	0.222	0.100	-	-	0.322	-
	Max	0.668	0.441	-	-	1.109	-
Early Upper Paleolithic Modern Human (n=7 for sTA and sCA, n=13 for sImax, sImin, and sJ)	Mean	0.402	0.266			0.668	-
	S.D.	0.094	0.062			0.152	-
	Min	0.283	0.195			0.478	-
	Max	0.587	0.400			0.926	-
East Eurasian Late Upper Paleolithic (n=7)	Mean	0.414	0.217			0.631	-
	S.D.	0.109	0.030			0.132	-
	Min	0.321	0.175			0.509	-
	Max	0.636	0.259			0.875	-

*Humeral lengths, body mass, and original properties used in calculating the standardizing properties are reported in Tables 1, except for ZKD humeri, where three length values were used (307.4, 315.7, and 324.0 mm).

Table 4(on next page)

Table 4

Table 4. Midshaft humeral standardized properties (by body mass x maximum length) of Zhoukoudian left humerus (II) and comparative samples*.

Table 4. Midshaft humeral standardized properties (by body mass x maximum length) of Zhoukoudian left humerus (II) and comparative samples*.

		sI_{max}	sI_{min}	sZ_{max}	sZ_{min}	sJ	sZ_p
ZKD Humerus II	(307.4)	0.424	0.251	0.039	0.031	0.675	0.061
	(315.7)	0.413	0.245	0.038	0.0306	0.658	0.060
	(324.0)	0.402	0.239	0.037	0.030	0.641	0.058
Tianyuan 1		0.213	0.139	0.022	0.017	0.352	0.033
Middle Paleolithic Modern Human	Mean	0.291	0.207			0.498	
(n=2)	S.D.	0.031	0.043			0.074	
	Min	0.269	0.177			0.446	
	Max	0.313	0.237			0.550	
Neanderthals	Mean	0.363	0.182			0.534	
(n=4 for sTA, sCA, and sJ, n=3 for sI_{max} and	S.D.	0.186	0.102			0.237	
sI_{min},)	Min	0.253	0.118			0.375	
	Max	0.578	0.300			0.877	
Early Upper Paleolithic Modern Human	Mean	0.300	0.201			0.506	
(n=9 for sTA and sCA, n=14 for sI_{max} and	S.D.	0.059	0.040			0.092	
sI_{min}, n=15 for sJ)	Min	0.202	0.129			0.355	
	Max	0.405	0.272			0.674	
East Eurasian Late Upper Paleolithic (n=5)	Mean	0.313	0.186			0.500	
	S.D.	0.044	0.035			0.077	
	Min	0.256	0.139			0.416	
	Max	0.353	0.215			0.566	

*Humeral lengths, body mass, and original properties used in calculating the standardizing properties are reported in Tables 2, except for ZKD humeri, where three length values were used (307.4, 315.7, and 324.0 mm).